MBNL1 required the UGCU motifs in the 5′ region of exon 17a (Figs 2B and 5B). As MBNL1 recognizes a UGCU motif to bind to its target pre-mRNA (Goers *et al.* 2010), it is anticipated that MBNL1 regulates the alternative splicing of exon 17a by its direct binding to *MYOM1* pre-mRNA. Although we did not test downregulation of MBNL1, the expanded CUG repeat increased the inclusion of exon 17a in a MBNL1-dependent manner (Fig. 2C), suggesting that abnormal splicing of *MYOM1* exon 17a in patients with DM1 may be due to the loss of MBNL function caused by trinucleotide repeat–mediated sequestering of MBNL proteins.

The essential UGCU motifs for MBNL1 regulation were located in the 5′ region of exon 17a. This is consistent with our previous study on the alternative splicing regulation of murine *Clcn1*, which revealed that MBNL1 bound to the 5′ end of exon 7A to repress its splicing. It has been suggested that the location of YGCY motifs in the flanking introns of the regulated exon determines whether MBNL1 promotes or suppresses splicing (Goers *et al.* 2010). In addition to this, our studies on alternative splicing of *Clcn1* and *MYOM1* revealed the importance of exonic region for MBNL1 function. Generally, in an exonic region, there are some regulatory elements named exonic splicing enhancer (ESE), which serve as binding sites for serine/arginine-rich (SR) proteins that facilitate the exon inclusion. So, we speculate that the interaction of MBNL1 with UGCU motifs may prevent SR proteins from binding to ESE in exon 17a and thus inhibit the exon inclusion in normal muscle. As shown in Fig. 5B, the mutation in the tandem UGCU motifs decreased the responsiveness to MBNL1, in that MBNL1 promoted the isoform D production; however, mut1 minigene responded to the over-expression of MBNL1 by increasing the ratio of isoform C. This result suggests that MBNL1 can influence the choice of 5′ splice sites of intron 17a. The production of isoform C was also promoted when the 5′ region of intron 17a was deleted (see Fig. 3, Δ5, data not shown). As there are several UGCU sequences in this deleted region, MBNL1 might bind to the 5′ region of intron 17a and prevent the usage of 5′ splice sites for isoform A and B.

In contrast to the result of MBNL proteins, the regulation of CELF proteins was inconsistent with the current pathomechanism of DM. Although the elevation of CELF1 and CELF2 has been observed in patients with DM1 (Timchenko *et al.* 1996), over-expression of either of the two proteins decreased the inclusion of exon 17a, that is, restored the splicing pattern in non-DM patients (Fig. 2B). Over-expression of CELF3 promoted strongly the inclusion of exon 17a; however, it is unlikely that CELF3 regulates *MYOM1* alternative splicing *in vivo* because CELF3 is expressed selectively in brain, and no expression of *CELF3* was detected by RT-PCR in DM1 cDNA used in this study (data not shown, and also see the study by Nezu *et al.* 2007). As MBNL1 and CELF1 regulate the alternative splicing of *MYOM1* to the same direction, we tried to dedicate the regulatory mechanisms of these two proteins. Remarkably, the minigene with mutations in the tandem UGCU motifs in exon 17a decreased responsiveness to MBNL1 but not to CELF1 (Fig. 5B,C), suggesting that CELF1 can regulate the *MYOM1* alternative splicing independently of the MBNL1 binding to its pre-mRNA. Furthermore, double expression of CELF1 and MBNL1 more suppressed the inclusion of exon 17a than those by the each protein (data not shown), which indicates the redundant function of MBNL1 and CELF1 in the regulation of the *MYOM1* alternative splicing. As CELF1 can repress the exon inclusion of *Tpm2*-ex17a minigene, it is likely that *cis*-element(s) for CELF1 may be located in exon 17a and its flanking introns. Actually, we found UGU-rich sequence around the boundary of intron 17 and exon 17a (Fig. 5A). Because we had previously shown that CELF1 bound specifically to UGU repeat RNA (Takahashi *et al.* 2000), the UGU-rich sequence might serve as a CELF1-binding site. When we think of the difference between CELF1 and MBNL1 in the regulation of the *MYOM1* alternative splicing, it is interesting that there were no UGU-rich regions around the *cis*-elements for MBNL1; the nearest UGU-rich region was 83 nt away from the UGCU motifs. Therefore, it is unlikely that MBNL1 and CELF1 may prevent the same SR protein from binding to *MYOM1* pre-mRNA. The identification of *cis*-element for CELF1 would be helpful to understand the regulation of the *MYOM1* alternative splicing; however, we plan to report the element in more detail in future.

Considering the fact that abnormal splicing of *MYOM1* exon 17a was observed in patients with DM1 (Fig 1B), the elevation of CELF1 and CELF2 might have little effect on exon 17a splicing in DM1 muscle. Actually, expression of the expanded CUG repeat prevented MBNL1 function but did not promote CELF1 activity (Fig. 2C). It is possible that DM480 might not express enough CUG repeat transcripts to lead hyperphosphorylation of CELF1 in our system; however, even so, the same level of

expression of DM480 sequestered MBNL1 and 'worsened' the splicing pattern of *MYOM1*. Thus, MBNL1 should be a main factor of the abnormal splicing of *MYOM1* in DM1 muscle.

In conclusion, we found the aberrant inclusion of *MYOM1* exon 17a as a novel splicing abnormality in DM1 skeletal muscle. This is an interesting example of the splicing abnormalities in DM1 because the alternative splicing of *MYOM1* is regulated by MBNL proteins and CELF1/2 to the same direction. Our results suggest that the abnormal behavior of CELF1/2 is negligible in aberrant splicing of *MYOM1* in patients with DM1; otherwise, another splicing factor may be involved with splicing abnormalities in DM1. Although comprehensive analysis using DNA microarray is a powerful tool to elucidate a broader network in DM1 pathomechanism, we only focused on one abnormal splicing event. There are several interesting candidates of splicing abnormalities in our microarray data. Surprisingly, only a few exons, including *LDB3/ZASP* exon 11, have been reported to be aberrantly spliced in patients with DM, and the other abnormal splicing events known to occur in patients with DM were not detected in this study. However, the probe signals for known abnormally spliced exons of *IR*, *CLCN1*, *SERCA1*, *MBNL1*, *MBNL2*, nebulin-related anchoring protein (*NRAP*) and dystrophin (*DMD*) showed changes consistent with previous reports, although the statistical significance of the changes did not satisfy our criterion, possibly due to the marked variability in DM abnormalities. Notably, a large portion of the mis-spliced candidates (13 exons) were related to the actin cytoskeleton, which may reflect the skeletal muscle histological abnormalities and muscle weakness of patients with DM1.

Experimental procedures

Tissue samples and RT-PCR

For RT-PCR validation, biopsied materials were obtained from the biceps brachii or quadriceps femoris of five patients with DM1 and five age-matched non-DM individuals without DM1-type histological abnormalities (Table S3 in Supporting Information). All clinical materials used in this study were obtained for diagnostic purposes with written informed consent. The studies were approved by the Ethical Committee. All biopsy samples were stored at −80 °C. Clinically, three of five patients with DM1 displayed a predominance of type 1 fibers. Clinical features of 'non-DM patients' are summarized in Table S3 in Supporting Information. Note that they were not diagnosed as any known myopathy including DM. Total RNA was extracted using the Trizol reagent (Invitrogen, Carlsbad, CA, USA) without DNase treatment. Typically, 0.5 μg of total RNA was reverse-transcribed for RT-PCR using a PrimeScript 1st Strand cDNA Synthesis kit (Takara Bio, Otsu, Japan) with random hexamer primers. Sequences of the primers used in RT-PCR for *MYOM1* (ex17a Fw and ex17a Rv) and *GAPDH* (GAPDH Fw and GAPDH Rv) are shown in Table S2 in Supporting Information. The products were electrophoretically resolved on an 8% polyacrylamide gel that was stained with ethidium bromide and analyzed using an LAS-3000 luminescence image analyzer (Fujifilm, Tokyo, Japan). The ratio of exon 17a inclusion in *MYOM1* was calculated as (17a inclusion)/(17a inclusion + 17a skipping) × 100 (see Fig. 1).

Microarray analysis

For microarray analysis, we used muscle samples from three patients with DM1 and four age-matched non-DM individuals (Table S3 in Supporting Information). Non-DM individuals were clinically diagnosed not as DM. Total RNA was extracted as described earlier, and its concentration and purity were calculated using NanoDrop ND-1000 (NanoDrop Technologies, Wilmington, DE, USA) and an Agilent 2100 Bioanalyzer (Agilent Technologies, Santa Clara, CA, USA). Total RNA samples were submitted to Kurabo Industries (Osaka, Japan; an authorized service provider for Affymetrix Japan K.K., Tokyo, Japan) for analysis using a GeneChip Human Exon 1.0 ST Array (Affymetrix Technologies) according to a standard protocol. The CEL files were further analyzed using exon array analyzer (Gellert *et al.* 2009), a web-based analytic tool, with the following criteria: probe set, core; algorithm, RMA; filters, default; *P*-value, <0.05; and SI, >1 or <−1. In this tool, gene level normalized intensity (NI) and SI are calculated as following: NI = (probe set intensity)/(expression level of the gene), SI = log 2 (NI_{DM1}/NI_{nonDM}) (Gellert *et al.* 2009).

Constructs

PCR-amplified fragments of *MYOM1* containing from exon 17 to exon 18 were cloned between the *Bsp*EI and *Eco*RI sites in pEGFP-C1 (Clontech, Mountain View, CA, USA). The genomic region covering exon 17 to exon 18 was divided into three fragments, and each fragment was amplified from human genomic DNA by PCR using pairs of primers MYOM1-1 to MYOM1-3 (Table S2 in Supporting Information). The first and second fragments were joined at the AccI site, and the second and third fragments at the *Xho*I site. To make intron-deleted minigenes, pairs of primers were designed to the flanking ends of the deleted regions. PCR products were gel-purified and circularized by self-ligation. Construction of pEGFP-Tpm2-ex1-2 vector and *Tpm2*-ex9 has been previously described (Kino *et al.* 2009). The chimeric minigenes of *Tpm2*-ex17a, 17a-9 and 9-17a were generated by insertion of PCR-amplified fragments into the pEGFP-Tpm2-

ex1-2 vector or *Tpm2*-ex9. For *Tpm2*-ex17a, a fragment corresponding to exon 17a and 100 bp of the both flanking introns was amplified from pMYOM1 with Tpm2-ex17a_Fw and Tpm2-ex17a_Rv, and this fragment was inserted between *Bgl*II and *Sal*I sites of pEGFP-Tpm2-ex1-2. The fragments for 17a-9 and 9-17a were amplified from *Tpm2*-ex17a with two primers complementary either to exon 17a (17a-9_R or 9-17a_F) or to pEGFP-C1 vector sequence (GFP-F or EGFP-C rv1). To insert these fragments into *Tpm2*-ex9, a *Bgl*II-recognition site in exon 9 and appropriate restriction sites in multicloning site were used. Because exon 17a would generate premature termination codons when ligated with exon 1, we inserted a cytosine nucleotide into exon 1 of *Tpm2*-ex17a and 17a-9 by PCR-based site-directed mutagenesis (Weiner & Costa 1994). Construction of the rest of the chimeric minigenes and site-directed mutagenesis of the pMYOM1 were performed using the PCR overlap extension method (Ho *et al.* 1989). A pair of primers with overlapping region was designed to the region around the junction of a chimeric minigene or the mutation site of a mutated minigene. The first round of PCR was carried out using each of the overlapping primers and each of two oligonucleotides complementary either to the 5′ or to 3′ ends of the minigene, to amplify overlapping portions of minigene from pMYOM1 or appropriate chimeric minigenes. Sequences of all the primers used in construction are shown in Table S2 in Supporting Information. The other constructs used in this study have been described previously (Kino *et al.* 2004, 2009; Nezu *et al.* 2007; Mori *et al.* 2008; Onishi *et al.* 2008). Briefly, the coding regions for the RNA-binding proteins were PCR-amplified from a human cDNA library and cloned into pSecDK, a mammalian expression vector with a myc-tag that was modified from pSecTagA (Invitrogen) to delete the Igκ chain leader sequence. The constructs have been confirmed to express intended proteins in a comparable level (Kino *et al.* 2009). DM18 and DM480 contain a fragment of the 3′ region of *DMPK* with a CTG18 and interrupted CTG480 repeats, respectively.

Cellular splicing assay

Cells transfected with plasmids for the expression of a protein and minigene were harvested 48 h post-transfection. Typically, cells were cultured in 12-well plates and transfected with 0.4 μg of protein expression plasmid (or cognate empty vector) and 0.1 μg of minigene expression plasmid using FuGENE6.0 (Roche Applied Sciences, Indianapolis, IN, USA). Total RNA was extracted with a GenElute Mammalian Total RNA Miniprep kit (Sigma-Aldrich, St. Louis, MO, USA) without DNase treatment. Typically, 1.0 μg of total RNA was reverse-transcribed with a PrimeScript 1st Strand cDNA Synthesis kit (Takara Bio) using oligo(dT) primers. PCR was performed using two oligonucleotides complementary to the EGFP sequence (GFP-F) and the last exon of minigene (ex17a Rv for pMYOM1 and deleted or mutated minigenes; Tpm2-Rv for chimeric minigenes), respectively. The products were electrophoretically resolved on an 8% polyacrylamide gel that was stained with ethidium bromide and analyzed using an LAS-3000 luminescence image analyzer.

Acknowledgements

We thank Dr H. Mitsuhashi for valuable discussions and encouragement. This work was supported by research grants from the Ministry of Health, Labor and Welfare, Japan (20B-13).

References

Agarkova, I., Auerbach, D., Ehler, E. & Perriard, J.C. (2000) A novel marker for vertebrate embryonic heart, the EH-myomesin isoform. *J. Biol. Chem.* **275**, 10256–10264.

Aslanidis, C., Jansen, G., Amemiya, C., *et al.* (1992) Cloning of the essential myotonic dystrophy region and mapping of the putative defect. *Nature* **355**, 548–551.

Bertoncini, P., Schoenauer, R., Agarkova, I., Hegner, M., Perriard, J.C. & Guntherodt, H.J. (2005) Study of the mechanical properties of myomesin proteins using dynamic force spectroscopy. *J. Mol. Biol.* **348**, 1127–1137.

Brook, J.D., McCurrach, M.E., Harley, H.G., *et al.* (1992) Molecular basis of myotonic dystrophy: expansion of a trinucleotide (CTG) repeat at the 3′ end of a transcript encoding a protein kinase family member. *Cell* **68**, 799–808.

Buxton, J., Shelbourne, P., Davies, J., Jones, C., Van Tongeren, T., Aslanidis, C., de Jong, P., Jansen, G., Anvret, M., Riley, B., Williamson, R. & Johnson, K. (1992) Detection of an unstable fragment of DNA specific to individuals with myotonic dystrophy. *Nature* **355**, 547–548.

Charlet, B.N., Savkur, R.S., Singh, G., Philips, A.V., Grice, E.A. & Cooper, T.A. (2002) Loss of the muscle-specific chloride channel in type 1 myotonic dystrophy due to misregulated alternative splicing. *Mol. Cell* **10**, 45–53.

Davis, B.M., McCurrach, M.E., Taneja, K.L., Singer, R.H. & Housman, D.E. (1997) Expansion of a CUG trinucleotide repeat in the 3′ untranslated region of myotonic dystrophy protein kinase transcripts results in nuclear retention of transcripts. *Proc. Natl Acad. Sci. USA* **94**, 7388–7393.

Du, H., Cline, M.S., Osborne, R.J., Tuttle, D.L., Clark, T.A., Donohue, J.P., Hall, M.P., Shiue, L., Swanson, M.S., Thornton, C.A. & Ares, M. Jr (2010) Aberrant alternative splicing and extracellular matrix gene expression in mouse models of myotonic dystrophy. *Nat. Struct. Mol. Biol.* **17**, 187–193.

Fardaei, M., Rogers, M.T., Thorpe, H.M., Larkin, K., Hamshere, M.G., Harper, P.S. & Brook, J.D. (2002) Three proteins, MBNL, MBLL and MBXL, co-localize in vivo with nuclear foci of expanded-repeat transcripts in DM1 and DM2 cells. *Hum. Mol. Genet.* **11**, 805–814.

Gellert, P., Uchida, S. & Braun, T. (2009) Exon Array Analyzer: a web interface for Affymetrix exon array analysis. *Bioinformatics* **25**, 3323–3324.

Goers, E.S., Purcell, J., Voelker, R.B., Gates, D.P. & Berglund, J.A. (2010) MBNL1 binds GC motifs embedded in pyrimidines to regulate alternative splicing. *Nucleic Acids Res.* **38**, 2467–2484.

Hao, M., Akrami, K., Wei, K., De Diego, C., Che, N., Ku, J.H., Tidball, J., Graves, M.C., Shieh, P.B. & Chen, F. (2008) Muscleblind-like 2 (Mbnl2) -deficient mice as a model for myotonic dystrophy. *Dev. Dyn.* **237**, 403–410.

Harley, H.G., Brook, J.D., Rundle, S.A., Crow, S., Reardon, W., Buckler, A.J., Harper, P.S., Housman, D.E. & Shaw, D.J. (1992) Expansion of an unstable DNA region and phenotypic variation in myotonic dystrophy. *Nature* **355**, 545–546.

Harper, P.S. (2001) *Myotonic Dystrophy*, 3rd edn. London: W. B. Saunders.

Hino, S., Kondo, S., Sekiya, H., Saito, A., Kanemoto, S., Murakami, T., Chihara, K., Aoki, Y., Nakamori, M., Takahashi, M.P. & Imaizumi, K. (2007) Molecular mechanisms responsible for aberrant splicing of SERCA1 in myotonic dystrophy type 1. *Hum. Mol. Genet.* **16**, 2834–2843.

Ho, S.N., Hunt, H.D., Horton, R.M., Pullen, J.K. & Pease, L.R. (1989) Site-directed mutagenesis by overlap extension using the polymerase chain reaction. *Gene* **77**, 51–59.

Ho, T.H., Bundman, D., Armstrong, D.L. & Cooper, T.A. (2005) Transgenic mice expressing CUG-BP1 reproduce splicing mis-regulation observed in myotonic dystrophy. *Hum. Mol. Genet.* **14**, 1539–1547.

Ho, T.H., Charlet, B.N., Poulos, M.G., Singh, G., Swanson, M.S. & Cooper, T.A. (2004) Muscleblind proteins regulate alternative splicing. *EMBO J.* **23**, 3103–3112.

Holt, I., Jacquemin, V., Fardaei, M., Sewry, C.A., Butler-Browne, G.S., Furling, D., Brook, J.D. & Morris, G.E. (2009) Muscleblind-like proteins: similarities and differences in normal and myotonic dystrophy muscle. *Am. J. Pathol.* **174**, 216–227.

Kalsotra, A., Xiao, X., Ward, A.J., Castle, J.C., Johnson, J.M., Burge, C.B. & Cooper, T.A. (2008) A postnatal switch of CELF and MBNL proteins reprograms alternative splicing in the developing heart. *Proc. Natl Acad. Sci. USA* **105**, 20333–20338.

Kanadia, R.N., Johnstone, K.A., Mankodi, A., Lungu, C., Thornton, C.A., Esson, D., Timmers, A.M., Hauswirth, W.W. & Swanson, M.S. (2003) A muscleblind knockout model for myotonic dystrophy. *Science* **302**, 1978–1980.

Kimura, T., Nakamori, M., Lueck, J.D., Pouliquin, P., Aoike, F., Fujimura, H., Dirksen, R.T., Takahashi, M.P., Dulhunty, A.F. & Sakoda, S. (2005) Altered mRNA splicing of the skeletal muscle ryanodine receptor and sarcoplasmic/endoplasmic reticulum Ca2+ -ATPase in myotonic dystrophy type 1. *Hum. Mol. Genet.* **14**, 2189–2200.

Kino, Y., Mori, D., Oma, Y., Takeshita, Y., Sasagawa, N. & Ishiura, S. (2004) Muscleblind protein, MBNL1/EXP, binds specifically to CHHG repeats. *Hum. Mol. Genet.* **13**, 495–507.

Kino, Y., Washizu, C., Oma, Y., Onishi, H., Nezu, Y., Sasagawa, N., Nukina, N. & Ishiura, S. (2009) MBNL and CELF proteins regulate alternative splicing of the skeletal muscle chloride channel CLCN1. *Nucleic Acids Res.* **37**, 6477–6490.

Kuyumcu-Martinez, N.M., Wang, G.S. & Cooper, T.A. (2007) Increased steady-state levels of CUGBP1 in myotonic dystrophy 1 are due to PKC-mediated hyperphosphorylation. *Mol. Cell* **28**, 68–78.

Lange, S., Agarkova, I., Perriard, J.C. & Ehler, E. (2005a) The sarcomeric M-band during development and in disease. *J. Muscle Res. Cell Motil.* **26**, 375–379.

Lange, S., Himmel, M., Auerbach, D., Agarkova, I., Hayess, K., Furst, D.O., Perriard, J.C. & Ehler, E. (2005b) Dimerisation of myomesin: implications for the structure of the sarcomeric M-band. *J. Mol. Biol.* **345**, 289–298.

Lin, X., Miller, J.W., Mankodi, A., Kanadia, R.N., Yuan, Y., Moxley, R.T., Swanson, M.S. & Thornton, C.A. (2006) Failure of MBNL1-dependent post-natal splicing transitions in myotonic dystrophy. *Hum. Mol. Genet.* **15**, 2087–2097.

Liquori, C.L., Ricker, K., Moseley, M.L., Jacobsen, J.F., Kress, W., Naylor, S.L., Day, J.W. & Ranum, L.P. (2001) Myotonic dystrophy type 2 caused by a CCTG expansion in intron 1 of ZNF9. *Science* **293**, 864–867.

Lueck, J.D., Lungu, C., Mankodi, A., Osborne, R.J., Welle, S.L., Dirksen, R.T. & Thornton, C.A. (2007) Chloride channelopathy in myotonic dystrophy resulting from loss of posttranscriptional regulation for CLCN1. *Am. J. Physiol.* **292**, C1291–C1297.

Mankodi, A., Logigian, E., Callahan, L., McClain, C., White, R., Henderson, D., Krym, M. & Thornton, C.A. (2000) Myotonic dystrophy in transgenic mice expressing an expanded CUG repeat. *Science* **289**, 1769–1773.

Mankodi, A., Takahashi, M.P., Jiang, H., Beck, C.L., Bowers, W.J., Moxley, R.T., Cannon, S.C. & Thornton, C.A. (2002) Expanded CUG repeats trigger aberrant splicing of ClC-1 chloride channel pre-mRNA and hyperexcitability of skeletal muscle in myotonic dystrophy. *Mol. Cell* **10**, 35–44.

Miller, J.W., Urbinati, C.R., Teng-Umnuay, P., Stenberg, M.G., Byrne, B.J., Thornton, C.A. & Swanson, M.S. (2000) Recruitment of human muscleblind proteins to (CUG)(n) expansions associated with myotonic dystrophy. *EMBO J.* **19**, 4439–4448.

Mori, D., Sasagawa, N., Kino, Y. & Ishiura, S. (2008) Quantitative analysis of CUG-BP1 binding to RNA repeats. *J. Biochem.* **143**, 377–383.

Nezu, Y., Kino, Y., Sasagawa, N., Nishino, I. & Ishiura, S. (2007) Expression of MBNL and CELF mRNA transcripts in muscles with myotonic dystrophy. *Neuromuscul. Disord.* **17**, 306–312.

Onishi, H., Kino, Y., Morita, T., Futai, E., Sasagawa, N. & Ishiura, S. (2008) MBNL1 associates with YB-1 in cytoplasmic stress granules. *J. Neurosci. Res.* **86**, 1994–2002.

Philips, A.V., Timchenko, L.T. & Cooper, T.A. (1998) Disruption of splicing regulated by a CUG-binding protein in myotonic dystrophy. *Science* **280**, 737–741.

Ranum, L.P. & Cooper, T.A. (2006) RNA-mediated neuromuscular disorders. *Annu. Rev. Neurosci.* **29**, 259–277.

Ranum, L.P. & Day, J.W. (2004) Myotonic dystrophy: RNA pathogenesis comes into focus. *Am. J. Hum. Genet.* **74**, 793–804.

Savkur, R.S., Philips, A.V. & Cooper, T.A. (2001) Aberrant regulation of insulin receptor alternative splicing is associated with insulin resistance in myotonic dystrophy. *Nat. Genet.* **29**, 40–47.

Schoenauer, R., Bertoncini, P., Machaidze, G., Aebi, U., Perriard, J.C., Hegner, M. & Agarkova, I. (2005) Myomesin is a molecular spring with adaptable elasticity. *J. Mol. Biol.* **349**, 367–379.

Sen, S., Talukdar, I., Liu, Y., Tam, J., Reddy, S. & Webster, N.J. (2010) Muscleblind-like 1 (Mbnl1) promotes insulin receptor exon 11 inclusion via binding to a downstream evolutionarily conserved intronic enhancer. *J. Biol. Chem.* **285**, 25426–25437.

Takahashi, N., Sasagawa, N., Suzuki, K. & Ishiura, S. (2000) The CUG-binding protein binds specifically to UG dinucleotide repeats in a yeast three-hybrid system. *Biochem. Biophys. Res. Commun.* **277**, 518–523.

Taneja, K.L., McCurrach, M., Schalling, M., Housman, D. & Singer, R.H. (1995) Foci of trinucleotide repeat transcripts in nuclei of myotonic dystrophy cells and tissues. *J. Cell Biol.* **128**, 995–1002.

Timchenko, L.T., Miller, J.W., Timchenko, N.A., DeVore, D.R., Datar, K.V., Lin, L., Roberts, R., Caskey, C.T. & Swanson, M.S. (1996) Identification of a (CUG)n triplet repeat RNA-binding protein and its expression in myotonic dystrophy. *Nucleic Acids Res.* **24**, 4407–4414.

Timchenko, N.A., Patel, R., Iakova, P., Cai, Z.J., Quan, L. & Timchenko, L.T. (2004) Overexpression of CUG triplet repeat-binding protein, CUGBP1, in mice inhibits myogenesis. *J. Biol. Chem.* **279**, 13129–13139.

Warf, M.B., Diegel, J.V., von Hippel, P.H. & Berglund, J.A. (2009) The protein factors MBNL1 and U2AF65 bind alternative RNA structures to regulate splicing. *Proc. Natl Acad. Sci. USA* **106**, 9203–9208.

Weiner, M.P. & Costa, G.L. (1994) Rapid PCR site-directed mutagenesis. *PCR Methods Appl.* **4**, S131–S136.

Received: 26 April 2011
Accepted: 8 June 2011

Supporting Information/Supplementary material

The following Supporting Information can be found in the online version of the article:

Figure S1 MBNL1 and CELF1 regulate *MYOM1* splicing in other cell lines.

Table S1 Microarray data

Table S2 Primer sequences

Table S3 Patient samples

Additional Supporting Information may be found in the online version of this article.

Please note: Wiley-Blackwell are not responsible for the content or functionality of any supporting materials supplied by the authors. Any queries (other than missing material) should be directed to the corresponding author for the article.

Journal of Neuroscience Research

Journal of Neuroscience Research 89:562–575 (2011)

Differential Effects of the HESR/HEY Transcription Factor Family on Dopamine Transporter Reporter Gene Expression Via Variable Number of Tandem Repeats

Kouta Kanno[1,2] **and Shoichi Ishiura**[1]*

[1]Department of Life Sciences, Graduate School of Arts and Sciences, The University of Tokyo, Tokyo, Japan
[2]Department of Biological Sciences, Graduate School of Science, The University of Tokyo, Tokyo, Japan

The 3′-untranslated region (UTR) of the human dopamine transporter (*DAT1*) gene contains a variable number of tandem repeats (VNTR) domain, which is thought to be associated with dopamine-related psychiatric disorders, personality, and behavior. However, the molecular and neuronal functions of polymorphisms within the VNTR domain are unknown. We previously identified the transcription factor HESR1 (HEY1) as a VNTR-binding protein. *Hesr1* knockout mice exhibit DAT up-regulation in the brain and low levels of spontaneous activity. Other members of the HESR (HEY) family, including HESR2 (HEY2) and 3 (HEYL), have similar DNA-binding domains. In this study, we analyzed the effects of HESR1, -2, and -3 on *DAT1* expression in human neuroblastoma SH-SY5Y cells using luciferase reporter assays. We found that the VNTR domain played an inhibitory role in *DAT1* reporter gene expression and that HESR1 and -2 inhibited expression via both the core promoter and the VNTR. The inhibitory effects of HESR family members on *DAT* reporter gene expression differed depending on the number of repeats in the VNTR domain. We also found that each Hesr was expressed in the dopaminergic neurons in the mouse midbrain. These results suggest that the HESR family is involved in *DAT* expression via the VNTR domain.

Key words: dopamine; genetic polymorphism; VNTR; luciferase reporter assay

The dopaminergic nervous system plays important regulatory roles in locomotion, cognition, reward, affection, and hormone release (Bannon et al., 2001; Jackson and Westlinddanielsson, 1994; Missale et al., 1998; Uhl, 2003). Thus, dopamine and its related genes are thought to be involved in neuropsychiatric disorders and behavioral traits. The human dopamine transporter (*DAT1*) gene is involved in many dopamine-related disorders. DAT levels are reduced in Parkinson's disease (PD) and elevated in attention deficit hyperactivity disorder (ADHD), Tourette's syndrome, and major depression (Madras et al., 1998; Muller-Vahl et al., 2000; Brunswick et al., 2003; Krause et al., 2003). In addition, several psychoactive drugs, including cocaine, amphetamine, and methylphenidate, are known to inhibit dopamine reuptake by DAT (Giros et al., 1991, 1992; Kilty et al., 1991; Shimada et al., 1991; Giros and Caron, 1993).

A functional genetic polymorphism has been described in the 3′-untranslated region (UTR) of exon 15 in *DAT1* (Michelhaugh et al., 2001). This 3′-UTR contains a 40-bp-long variable number of tandem repeats (VNTR) domain (Fig. 1; Vandenbergh et al., 1992; Michelhaugh et al., 2001). The polymorphism within this region is known to be associated with such neuropsychiatric disorders as ADHD, PD, alcoholism, and drug abuse (Cook et al., 1995; Ueno et al., 1999; Vandenbergh et al., 2000; Ueno, 2003; D'souza and Craig, 2008) and with modified gene expression depending on the genotype in vivo (Heinz et al., 2000; Jacobsen et al., 2000; Mill et al., 2002; D'souza and Craig, 2008) and in mammalian cell lines (Fuke et al., 2001, 2005; Inoue-Murayama et al., 2002; Miller and Madras, 2002; Greenwood and Kelsoe, 2003; Mill et al., 2005; VanNess et al., 2005; D'souza and Craig, 2008). It is expected that this region contains binding sites for interacting proteins, but, because these factors have not been described, the molecular and neuronal functions of the polymorphism are unknown (Michelhaugh et al., 2001).

We previously identified and characterized HESR1 (HEY1) as a *trans*-acting repressor of gene expression

Contract grant sponsor: Human Frontier Science Program; Contract grant sponsor: Ministry of Education, Culture, Sports, Science, and Technology of Japan; Contract grant sponsor: JSPS Research Fellowship for Young Scientists (to K.K.).

*Correspondence to: Dr. Shoichi Ishiura, Department of Life Sciences, Graduate School of Arts and Sciences, The University of Tokyo, 3-8-1, Komaba, Meguro-ku, Tokyo 153-8902, Japan.
E-mail: cishiura@mail.ecc.u-tokyo.ac.jp

Received 18 August 2010; Revised 10 November 2010; Accepted 9 December 2010

Published online 2 February 2011 in Wiley Online Library (wileyonlinelibrary.com). DOI: 10.1002/jnr.22593

that acts through the 3′-UTR of *DAT1* via a yeast one-hybrid system (Fuke et al., 2005). In addition, we also showed that HESR1 binds directly to the region by electrophoretic mobility shift assay (EMSA) and represses the expression of the endogenous *DAT1* gene in the HEK293 cell line by RT-PCR assay (Fuke et al., 2006). In *Hers1* knockout (KO) mice, *DAT1* expression was enhanced, and the mice exhibited a reduction in spontaneous locomotor activity and exploration to novelty (Fuke et al., 2006). These findings suggest that the human *HESR1* gene and the polymorphisms could be related to many psychiatric disorders and behavioral traits. However, it is possible that other factors affect *DAT1* expression via the VNTR domain, insofar as more than one interacting factor is expected to bind this region (Michelhaugh et al., 2001). Conflicting results have been reported from studies using different cell lines, which may express different transcription factors (Fuke et al., 2001, 2005; Inoue-Murayama et al., 2002; Miller and Madras, 2002; Greenwood and Kelsoe, 2003; Mill et al., 2005; VanNess et al., 2005; D'souza and Craig, 2008). These results suggest that *DAT1* expression can be altered by cell-specific factors depending on the VNTR alleles present.

The Hesr family genes *Hesr1*, *-2*, and *-3* (*Hey1*, *Hey2*, and *HeyL*) were identified as the hairy/enhancer split-type basic helix-loop-helix (bHLH) genes. They have been shown to be direct transcriptional targets of the Notch signaling pathway, which is essential for neural development (Kokubo et al., 1999; Leimeister et al., 1999; Nakagawa et al., 1999; Henderson et al., 2001; Iso et al., 2001, 2003; Wang et al., 2002; Sakamoto et al., 2003). HESR family genes carry a bHLH domain essential for DNA binding as well as an Orange domain and YRPW motif, which mediate interaction with proteins and affect dimerization or recruitment of corepressors (Fischer and Gessler, 2007; Fig. 2). HESR proteins repress the expression of target genes by binding to E- or N-box bHLH-binding consensus sites (Nakagawa et al., 2000; Iso et al., 2001, 2003). The bHLH domain is highly conserved among HESR family members (Steidl et al., 2000), and Hesr1 and -2 repress gene expression via the same sequence (Kokubo et al., 2007). Thus, HESR1 along with HESR2 and -3 may be candidate factors regulating *DAT* expression via the VNTR. However, any roles of HESR2 and -3 in *DAT* gene expression have not yet been characterized.

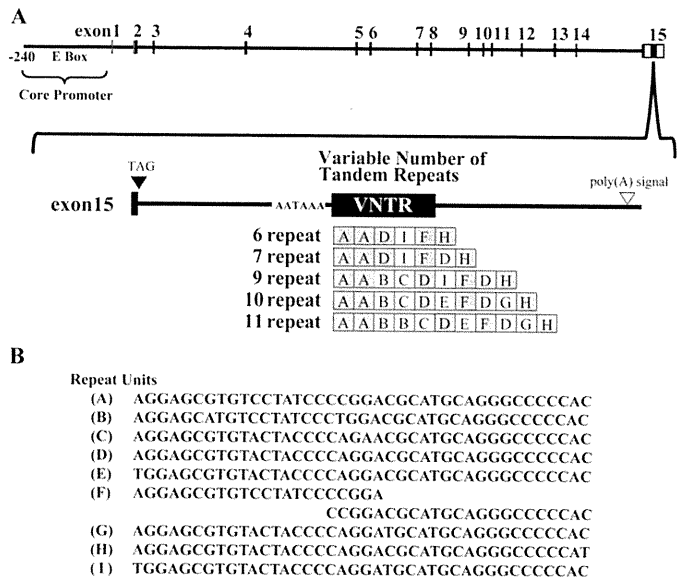

Fig. 1. Genomic structure of *DAT1* and allelic variants of the VNTR domain in exon 15. **A:** The coding region (black box), noncoding region (open box), VNTR domain, and constant parts of the repeat units (gray box) are shown. Exon 15 of *DAT1* contains a stop codon (solid arrowhead) and polyadenylation signal (open arrowhead). Upstream of the VNTR domain are six nucleotides (AATAAA) that resemble a polyadenylation signal. The allelic variants of the VNTR indicate the repeat unit type (A–I) for each allele. **B:** Nucleotide sequence of each unit of the VNTR polymorphism in the 3′-UTR of *DAT1*.

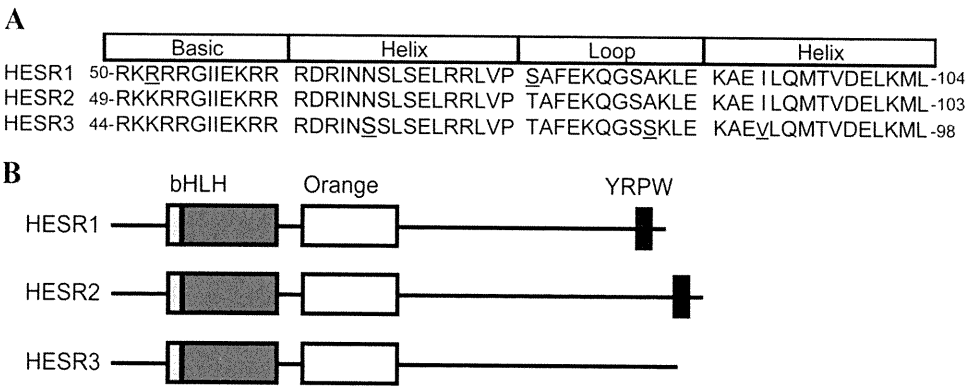

Fig. 2. Structure of HESR family members. **A:** Comparison of the primary sequences of the bHLH domain among human HESR family members (HESR1, 50–104 amino acids; HESR2, 49–103 amino acids; and HESR3, 44–98 amino acids). Those residues that differ among the family members are underscored. The primary sequences of the bHLH domain in the mouse Hesr family are identical to those in the human protein. **B:** Structure of the HESR family with the three major domains noted: bHLH domain, Orange domain, and YRPW motif.

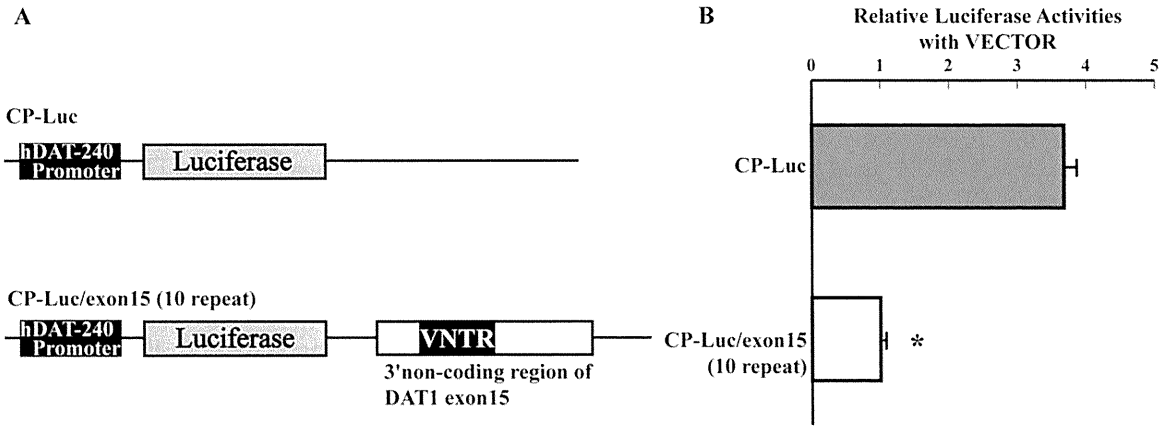

Fig. 3. Luciferase reporter vector and its activity in SY-SH5Y cells. **A:** Schematic diagram of the luciferase reporter vectors CP-Luc and CP-Luc/exon 15. CP-Luc contains only the *DAT* core promoter, whereas CP-Luc/exon 15 contains both the core promoter and the 3′-UTR with 10r, which is the most common allele. **B:** Negative regulation of gene expression through the 3′-UTR of *DAT* in SY-SH5Y cells. CP-Luc or CP-Luc/exon 15 and empty vector were transfected into the cells. Relative luciferase activity is expressed as the mean ± SEM. $^*P < 0.0001$, Student's *t*-test.

In this study, we sought to clarify whether HESR2 and -3, as well as HESR1, also affect *DAT1* expression in human neuroblastoma cells via the 3′-UTR, including the VNTR region. Luciferase reporter constructs were made containing the endogenous *DAT1* core promoter and the VNTR with 6, 7, 9, 10, or 11 repeats, which is consistent with the sequences reported previously (Fuke et al., 2001). The differential effects on VNTR among HESR1, -2, and -3 were also characterized. Furthermore, we conducted immunohistochemistry for Hesrs and tyrosine hydroxylase (TH), a marker of dopaminergic neurons, in mouse midbrains to analyze localization of Hesr proteins for the investigation of HESR family function in the brain dopamine systems, because localization of HESR proteins in the adult brain has not been reported, although dopaminergic neurons localize in the specific brain regions (Bjorklund and Dunnett, 2007).

MATERIALS AND METHODS

General Procedure

First, to characterize the role of the 3′-UTR in *DAT* expression, a CP-Luc or CP-Luc/exon15 (10r) reporter vector and empty vector (control) were expressed in cells. Ten repeats is the most common allele in the population (Fuke et al., 2005; D'souza and Craig, 2008). CP-Luc contained only the *DAT* core promoter, whereas CP-Luc/exon15 contained both the core promoter and the 3′-UTR (Fig. 3). Next, the empty vector or each HESR was cotransfected with CP-Luc or CP-Luc/exon15 (10r). Finally, to compare the VNTR alleles and HESRs, each repeat (6, 7, 9, 10, or 11r) of CP-Luc/exon15 and the HESR or vector were cotransfected. The relative luciferase activity was standardized to that of the vector. In the experiment examining the repeat effect, the relative luciferase activity was standardized to that of 10r in each group. In addition, the localization of Hesrs in the mouse midbrain was detected by immunohistochemistry.

Cloning and Construction

Two kinds of luciferase reporter vectors were prepared: CP-Luc and CP-Luc/exon 15 (see Fig. 3A). CP-Luc contained the human *DAT* core promoter (–240 to +2; Fig. 1A; Kouzmenko et al., 1997; Sacchetti et al., 1999) cloned from the DAT1-8317 plasmid (Sacchetti et al., 1999), a gift from Dr. Michael J. Bannon (Wayne State University, School of Medicine, Detroit, MI), upstream of the firefly luciferase site in the modified pGL3 vector (Promega, Madison, WI). CP-Luc/exon 15 contained the human *DAT* core promoter and 3′-UTR region including the VNTR domain downstream of the luciferase site in CP-Luc. There are five kinds of VNTR alleles (6, 7, 9, 10, and 11r), which is consistent with the sequence (Fig. 1B) reported in our previous study (Fuke et al., 2001). These reporter vectors are the same as the constructs used in our previous study (Fuke et al., 2005); schematic structures of the reporter vectors are shown in Figure 3A. Additional information on these constructs is described in our previous work (Fuke et al., 2005).

All of the HESR family expression vectors were made by cloning the cDNA into myc-pcDNA modified from pcDNA 3.1+ (Invitrogen, Carlsbad, CA), an expression vector for mammalian cell lines. The Myc-tag is located upstream of the multicloning site. Myc-pcDNA was also used as a control vector (the vector described in Figs. 3–6). Myc-pcDNA and Myc-HESR1 (human) are the same as the constructs described in our previous study (Fuke et al., 2005). Myc-Hesr1 (mouse) was a gift from Dr. Hiroki Kokubo (Division of Mammalian Development, National Institute of Genetics, Mishima, Japan). Human HESR2 and -3 cDNAs were amplified from a fetal brain cDNA library (Clontech, Palo Alto, CA) by PCR with oligonucleotide primers and the high-fidelity DNA polymerase PrimeStar (TaKaRa, Shiga, Japan). Mouse Hesr2 and -3 cDNAs were amplified from cloned cDNAs in pBluescript (gifts from Dr. Hiroki Kokubo) by PCR with oligonucleotide primers and PrimeStar (TaKaRa). Each oligonucleotide primer was designed to

contain a restriction site (italicized). The primer sequences are as follows: human HESR2, Fw (XhoI) 5′-TTA*CTCGAG*AT GAAGCGCCC-3′ and Rv (ApaI) 5′-TTA*GGGCCC*T TAAAAAGCTCCAAC-3′; human HESR3, Fw (XhoI) 5′-TTA*CTCGAG*ATGAAGCGACCC-3′ and Rv (XhoI) 5′-TTA*CTCGAG*TCAGAAAGCCCC-3′; mouse Hesr2, Fw (XhoI) 5′-TTA*CTCGAG*ATGAAGCGCCCT-3′ and Rv (ApaI) 5′-ATAGGGCCCTTAAAAGCTGGCTCC-3′; and mouse Hesr3, Fw (XhoI) 5′-TTA*CTCGAG*ATGAA GCGGCC-3′ and Rv (ApaI) 5′-TTAGGGCCCTCAGAAA GCC-3′. These amplified fragments were cloned into T-Vectors (Promega p-GEM T Easy Kit) and sequenced by the dideoxy chain termination method with CEQ DTCS and CEQ8000 (Beckman Coulter, Brea, CA). Finally, the fragments were digested with each restriction enzyme and subcloned into myc-pcDNA.

Cell Culture and Transient Transfection: Luciferase Reporter Assay

The methods used for culture, transfection, cell harvesting, and luciferase activity measurements followed the standard methods of the Dual-Luciferase Reporter Assay System (Promega). SH-SY5Y cells were cultured in Dulbecco's modified Eagle's medium (DMEM; Sigma, St. Louis, MO) supplemented with 10% FBS at 37°C in an atmosphere of 5% CO_2. SH-SY5Y cells were plated into 24-well plates and cultured until they grew to 80% confluence before transfection. The cells were transfected with 1 μg total plasmid using Lipofectamine 2000 reagent (Invitrogen). The firefly luciferase reporter gene (0.5 μg) and each HESR or vector (0.5 μg) were coexpressed in the cells. Plasmid pRL (Promega) containing the sea pansy luciferase gene was cotransfected (20 ng) as an internal control to normalize the transfection efficiency in all experiments. After 48 hr, the cells were harvested and stored at −80°C. Luciferase activity was assayed using the Dual-Luciferase Reporter Assay System (Promega). The firefly and sea pansy luciferase activity was measured using a Centro LB 960 (Berthold, Bad Wildbad, Germany) for 10 sec after a 2-sec delay, and then the value of each sample was calculated as light units of firefly luciferase per that of sea pansy. Each HESR group and its controls were measured at the same time on a Centro LB 960.

Animals

Adult (9-week-old) male C57BL6/J mice (CLEA Japan, Tokyo, Japan) were kept under a controlled temperature (23–25°C) and photoperiod (LD 14:10, lights off at 22:00 hr). Food and water were available freely. All experiments were conducted according to the Regulations for Animal Experimentation at the University of Tokyo (Tokyo, Japan).

Tissue Preparation

The mice were deeply anesthetized using sodium pentobarbital (50 mg/kg body weight) and then perfused intracardially with 0.05 M phosphate-buffered saline (PBS; pH 7.4) followed by 4% paraformaldehyde in 0.05 M phosphate buffer (PB). The brains were removed and postfixed with the same fixative for 2 hr and immersed in 30% sucrose in 0.05 M PB for several days at 4°C. Serial coronal brain sections (20 μm) including the midbrain ventral tegmental area (VTA) and substantia nigra (SN; −3.04 to −3.49 to the bregma) were made with a cryostat and collected according to a brain map (Franklin and Paxinos, 2008). Five animals were used in this experiment.

Immunohistochemistry

Immunoperoxidase staining. Free-floating sections of the midbrain were incubated with 0.6% H_2O_2 in 10 mM PBS for 30 min at room temperature (RT) before and after rinsing with 10 mM PBS. Next, the sections were incubated with 5% normal goat serum (NGS; Vector Laboratories, Burlingame, CA), 0.4% Triton X-100, and 10 mM PBS for 1 hr at RT and then with a primary rabbit antibody against Hesr1 (working dilution 1:500; Chemicon, Temecula, CA), Hesr2 (1:1,000; Chemicon), or Hesr3 (1:500; Chemicon) containing 5% NGS, 0.4% Triton X-100, and 10 mM PBS for 3 nights at 4°C. After washing with 10 mM PBS, the sections were reacted with biotinylated goat anti-rabbit IgG (1:200; Vector Laboratories) in 5% NGS, 0.4% Triton X-100, and 10 mM PBS overnight at 4°C. The sections were rinsed with 10 mM PBS three times and then incubated in avidin-biotin-peroxidase complex (ABC) solution (Vectastain Elite ABC Kit; Vector Laboratories). Next, the sections were reacted with 0.05% 3,3′-diaminobenzidine (DAB) in 0.01% H_2O_2 and 100 mM Tris-HCl to visualize Hesr1-, -2-, or -3-immunoreactive (-ir) cells.

For single staining of the TH-ir (a marker of dopaminergic neurons) cells, similar steps were taken, except for the steps involving incubation with the primary or secondary antibody and visualization. The sections were incubated with a mouse anti-TH antibody (1:10,000; Chemicon) overnight at 4°C. The sections were then reacted with biotinylated goat anti-mouse IgG (1:200, Vector Laboratories) in 5% NGS, 0.4% Triton X-100, and 10 mM PBS overnight at 4°C after washing with 10 mM PBS three times. The sections were rinsed with 10 mM PBS three times and then incubated in ABC solution (Vector Laboratories). Next, the sections were reacted with 0.02% DAB solution to visualize TH-ir cells.

For double labeling, the same staining steps as for TH were performed after staining for each Hesr. Instead of DAB, a Vector SG Kit was used for visualization of TH after the ABC reaction. Immunostained sections mounted on slides were dehydrated through a graded ethanol series, cleared with xylene, and then coverslipped with an embedding agent.

Fluorescence immunohistochemistry for Hesrs and TH. Free-floating sections were rinsed with 10 mM PBS. The sections were then incubated with 5% normal donkey serum (NDS; Jackson Immunoresearch, West Grove, PA), 0.4% Triton X-100, and 10 mM PBS for 1 hr at RT and then with the primary rabbit antibody against Hesr1 (1:500; Chemicon), Hesr2 (1:1,000; Chemicon), or Hesr3 (1:500; Chemicon) and the primary mouse antibody for TH (1:10,000; Chemicon) in 5% NDS, 0.4% Triton X-100, and 10 mM PBS for 2 nights at 4°C. After washing with 10 mM PBS, the sections were reacted with donkey anti-rabbit IgG (1:200; Jackson Immunoresearch; Cy3) and donkey anti-mouse IgG (1:200; Jackson Immunoresearch; Cy2) in 5% NDS, 0.4% Triton X-100, and 10 mM PBS overnight at

4°C. Next, the sections were rinsed with 10 mM PBS before and after incubating with Hoechst 33342 (1:1,000; Dojindo, Tokyo, Japan) for 15 min. The immunostained sections were mounted on slides and then coverslipped. Images were captured with a digital CCD camera (DP70; Olympus, Tokyo, Japan) and the microscope software manager DP (Olympus) and analyzed in Photoshop CS4 (Adobe, San Jose, CA).

Statistical Analysis

Statistical analysis was performed in JMP 8.0 (SAS Institute). All values are reported as the mean ± SEM. Each value was standardized to that of CP-Luc/exon15 (10r) (Fig. 3), vector (Figs. 4, 5), or 10r (Fig. 6) in each group. Student's *t*-test was performed to detect statistical significance between two experimental objects. Tukey-Kramer's honestly significant difference (HSD) test was used as a post hoc test after one-way ANOVA. Tukey-Kramer's HSD test is a standard method of JMP to find significant difference among data after ANOVA. In addition, two-way ANOVA was conducted to detect interactive effects between the number of VNTR repeats and HESRs. Differences were considered significant at $P < 0.05$.

RESULTS

Lusciferase Activity of CP-Luc and CP-Luc/Exon15 (10r) in SH-SY5Y Cells

To determine the effect of the VNTR domain on *DAT1* expression, we made luciferase reporter constructs (Fig. 3). The relative luciferase activity of CP-Luc was 3.68 ± 0.15, whereas that of CP-Luc/exon 15 (10r) was 1.00 ± 0.03. A significant difference was noted between CP-Luc and CP-Luc/exon 15 (10r) ($P < 0.0001$, n = 8; Fig. 3). These results indicate that the 3′-UTR including the VNTR domain strongly inhibited luciferase expression in this reporter assay.

Effects of Human HESR and Mouse Hesr Family on Lusciferase Activity of CP-Luc

We next examined the effect of HESR family members on expression of the CP-Luc plasmid (Fig. 4A).

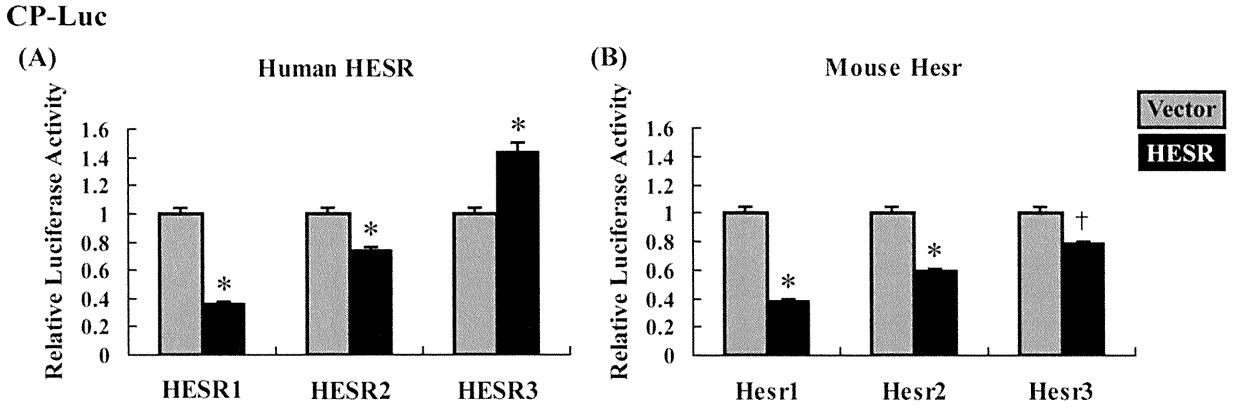

Fig. 4. Effects of the HESR family on the luciferase activity of CP-Luc. Cells were transfected with the CP-Luc reporter construct and human (**A**) and mouse (**B**) Hesrs or with empty vector. The values represent the mean ± SEM. of relative luciferase activity of the reporter construct in each group. *$P < 0.0001$ vs. vector, †$P < 0.0003$ vs. vector, Student's *t*-test.

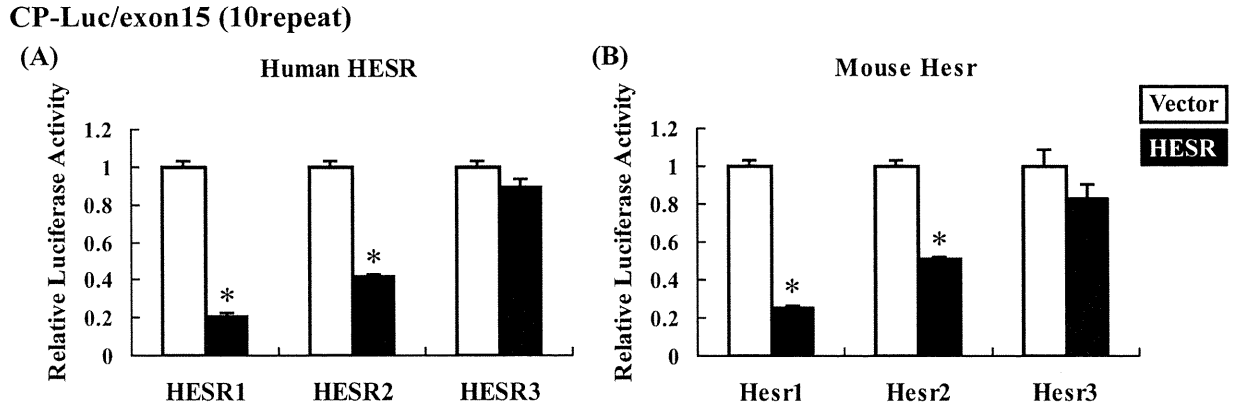

Fig. 5. Effects of the HESR family on the luciferase activity of CP-Luc/exon 15 (10r). Cells were transfected with CP-Luc/exon 15 (10r) and human (**A**) and mouse (**B**) Hesrs or with empty vector. The values represent the mean ± SEM. of relative luciferase activity of the reporter construct in each group. *$P < 0.0001$ vs. vector, Student's *t*-test.

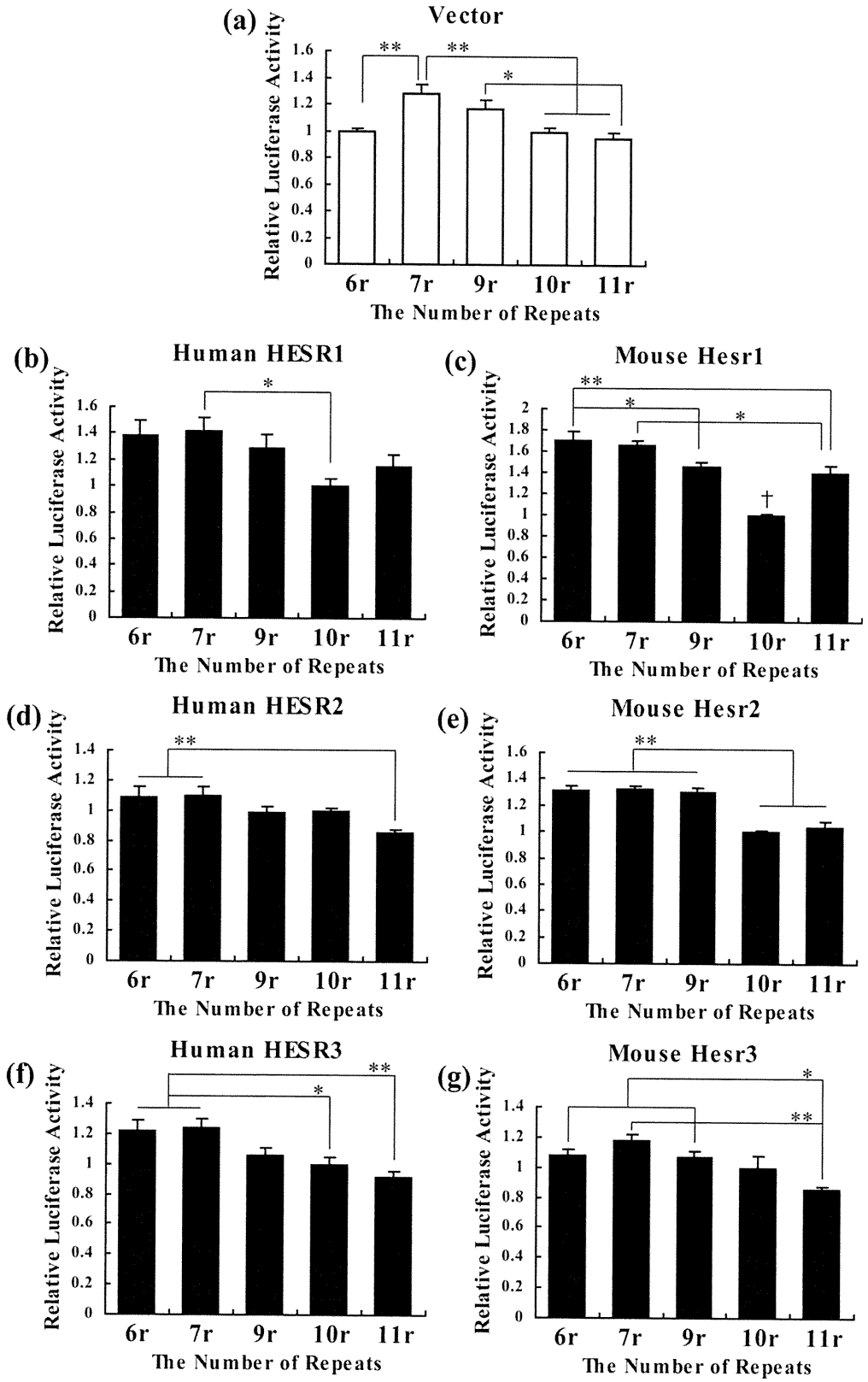

Fig. 6. Differential effects of the HESR family on the VNTR alleles. Cells were transfected with CP-Luc/exon 15 containing the indicated number of repeats and human (**b,d,f**) or mouse Hesrs (**c,e,g**) or with empty vector (**a**). Relative luciferase activity is expressed as the mean ± SEM. of relative luciferase activity of the reporter construct in each group. $^{*}P < 0.05$, $^{**}P < 0.01$, $\dagger P < 0.01$ vs. the other repeats, Tukey-Kramer's HSD test after one-way ANOVA.

With the expression of human HESR family members, the luciferase activity of CP-Luc relative to the vector control (1.00 ± 0.04) was as follows: HESR1, 0.36 ± 0.01; HESR2, 0.74 ± 0.02; and HESR3, 1.44 ± 0.06. The activity of CP-Luc with HESR1 or 2 was significantly lower than that with the vector control ($P < 0.0001$, n = 8 in each group), whereas that with HESR3 was higher than the control ($P < 0.0001$, n = 8 in each group).

With the expression of mouse Hesr family members (Fig. 4B), the luciferase activity of CP-Luc relative to the vector control (1.00 ± 0.04) was as follows: Hesr1, 0.39 ± 0.01; Hesr2, 0.60 ± 0.01; and Hesr3, 0.79 ± 0.01. The activity of CP-Luc with Hesr1 ($P < 0.0001$), -2 ($P < 0.0001$), or -3 ($P < 0.0003$) was significantly lower than with the vector (n = 8 in each group). These results indicate that only human HESR3 stimulated the expression of the CP-Luc construct containing the human *DAT1* core promoter, whereas expression of the other family members inhibited expression.

Effects of Human HESR and Mouse Hesr Family on Lusciferase Activity of CP-Luc/Exon 15 (10r)

To investigate the role of the VNTR domain, we cotransfected HESR genes with CP-Luc/exon 15 (10r). With the expression of human HESR family members (Fig. 5A), the luciferase activity of the CP-Luc/exon 15 (10r) relative to the vector control (1.00 ± 0.03) was as follows: HESR1, 0.21 ± 0.01; HESR2, 0.42 ± 0.01; and HESR3, 0.90 ± 0.04. These results illustrate that the luciferase activity of CP-Luc/exon 15 (10r) with HESR1 or 2 was significantly lower than with the vector ($P < 0.0001$, n = 8 in each group), although no significant decrease was observed with HESR3 ($P = 0.07$, n = 8).

The same trend was observed for mouse Hesr (Fig. 5B). With the expression of mouse Hesr family proteins, the luciferase activity of CP-Luc/exon 15 (10r) with each Hesr relative to the vector control (1.00 ± 0.07) was as follows: Hesr1, 0.25 ± 0.01; Hesr2, 0.51 ± 0.01; and Hesr3, 0.83 ± 0.09. The level of luciferase activity with Hesr1 or -2 was significantly lower than that with the vector ($P < 0.0001$, n = 8 in each group), whereas no significant decrease in activity was detected with Hesr3 ($P = 0.16$, n = 7).

Comparison of Effects of HESR Family and VNTR on Lusciferase Activity of CP-Luc/Exon15 (nr)

We investigated the effect of human and mouse HESR family members on the VNTR domain by first evaluating the effect of the repeat number. Luciferase expression from the CP-Luc/exon 15 construct is shown in Figure 6a. The following levels of activity were calculated: 6r, 0.99 ± 0.02; 7r, 1.28 ± 0.06; 9r, 1.16 ± 0.07; 10r, 1.00 ± 0.03; and 11r, 0.95 ± 0.04. One-way ANOVA indicated that there was a significant effect of the number of repeats ($F_{4,35} = 8.0167$, $P < 0.0001$). Post hoc analysis indicated that the luciferase activity level associated with 7r was significantly higher than that with 6, 10, or 11r ($P < 0.01$) and that the level of activity associated with 9r was significantly higher than that associated with 11r ($P < 0.05$; n = 8 in each group; Fig. 6a).

The effect of human HESR1 on the VNTR repeat number is shown in Figure 6b. With the expression of HESR1, CP-Luc/exon 15 activity (6r, 1.38 ± 0.11; 7r, 1.41 ± 0.11; 9r, 1.29 ± 0.11; 10r, 1.00 ± 0.06; and 11r, 1.14 ± 0.10) was compared with that for the vector alone (6r, 4.69 ± 0.11; 7r, 6.06 ± 0.28; 9r, 5.48 ± 0.35; 10r, 4.72 ± 0.16; and 11r, 4.50 ± 0.19). One-way ANOVA indicated a significant effect of the number of repeats ($F_{4,34} = 3.006$, $P < 0.032$). Post hoc analysis indicated that the luciferase activity associated with 7r was significantly higher than that associated with 10r (n = 7 for 11r, n = 8 in the other groups; Fig. 6b). In addition, two-way ANOVA indicated that there was a significant interaction between the number of repeats with HESR1 (or vector) ($F_{4,69} = 5.04$, $P < 0.002$).

We also investigated the effects of mouse Hesr1 (Fig. 6c). With the expression of Hesr1, CP-Luc/exon 15 activity (6r, 1.70 ± 0.08; 7r, 1.65 ± 0.05; 9r, 1.46 ± 0.04; 10r, 1.00 ± 0.02; and 11r, 1.41 ± 0.06) was compared with the control vector (6r, 3.90 ± 0.09; 7r, 5.04 ± 0.23; 9r, 4.56 ± 0.29; 10r, 3.92 ± 0.13; and 11r, 3.74 ± 0.16). As shown for human HERS1, one-way ANOVA indicated that there was a significant effect of the number of repeats ($F_{4,35} = 25.7587$, $P < 0.0001$). Post hoc analysis indicated that the level of luciferase activity associated with 6r was significantly higher than that associated with 9r ($P < 0.05$) or 11r ($P < 0.01$), and that the level for 7r was also higher than that for 11r (0.05). Furthermore, the lowest level of activity was observed for 10r ($P < 0.01$, n = 8 in each group; Fig. 6c). In addition, two-way ANOVA indicated that there was a significant interaction between the number of repeats with Hesr1 or the control vector ($F_{4,70} = 6.34$, $P < 0.002$).

We also investigated the effects of human HESR2 and mouse Hesr2. With the expression of human HERS2, CP-Luc/exon 15 activity (6r, 1.08 ± 0.07; 7r, 1.10 ± 0.06; 9r, 0.99 ± 0.04; 10r, 1.00 ± 0.02; and 11r, 0.85 ± 0.02) was again compared with the control vector (6r, 2.36 ± 0.05; 7r, 3.05 ± 0.14; 9r, 2.76 ± 0.17; 10r, 2.36 ± 0.08; and 11r, 2.26 ± 0.10) (Fig. 6d). One-way ANOVA indicated that there was a significant effect of the number of repeats ($F_{4,35} = 4.6640$, $P < 0.004$). Post hoc analysis indicated that the level of luciferase activity associated with 6 or 7r was significantly higher than that associated with 11r ($P < 0.01$, n = 8 in each group; Fig. 6d). In addition, two-way ANOVA indicated that there was a significant interaction between the number of repeats with HESR2 (or the control vector) ($F_{4,70} = 5.29$, $P < 0.0009$).

With the expression of mouse Hesr2 (Fig. 6e), CP-Luc/exon15 activity (6r, 1.32 ± 0.02; 7r, 1.32 ± 0.03; 9r, 1.30 ± 0.03; 10r, 1.00 ± 0.01; and 11r, 1.04 ± 0.04) was again compared with the control vector (6r, 1.94 ± 0.04; 7r, 2.51 ± 0.11; 9r, 2.26 ± 0.14; 10r,

1.95 ± 0.07; and 11r, 1.86 ± 0.08). One-way ANOVA indicated that there was a significant effect of the number of repeats ($F_{4,35}$ = 31.6769, $P < 0.0001$). Post hoc analysis indicated that the level of luciferase activity for 6, 7, or 9r was significantly higher than that for 10 or 11r ($P < 0.01$, n = 8 in each group; Fig. 6e). In addition, two-way ANOVA indicated that there was a significant interaction between the number of repeats with Hesr2 (or the control vector; F*4, 70* = 4.19, $P < 0.0045$).

Human HESR3 and mouse Hesr3 were also investigated. With human HESR3 expression, CP-Luc/exon 15 activity (6r, 1.22 ± 0.07; 7r, 1.24 ± 0.06; 9r, 1.06 ± 0.05; 10r, 1.00 ± 0.04; and 11r, 0.92 ± 0.04) was compared with the control vector (6r, 1.11 ± 0.03; 7r, 1.43 ± 0.07; 9r, 1.29 ± 0.08; 10r, 1.12 ± 0.04; and 11r, 1.06 ± 0.05). One-way ANOVA again indicated a significant effect of the number of repeats ($F_{4,35}$ = 7.0211, $P < 0.0003$). Post hoc analysis indicated that the level of luciferase activity using 6r or 7r was significantly higher than that using 10 ($P < 0.05$) or 11r ($P < 0.01$; n = 8 in each group; Fig. 6f). In addition, two-way ANOVA indicated that there was a significant interaction between the number of repeats with HESR3 or control vector ($F_{4,70}$ = 3.14, $P < 0.02$).

With the expression of mouse Hesr3, CP-Luc/exon 15 activity (6r, 1.08 ± 0.04; 7r, 1.18 ± 0.04; 9r, 1.07 ± 0.04; 10r, 1.00 ± 0.08; and 11r, 0.85 ± 0.03) was again compared with that of the control vector (6r, 1.15 ± 0.07; 7r, 1.44 ± 0.07; 9r, 1.28 ± 0.05; 10r, 1.20 ± 0.10; and 11r, 1.07 ± 0.05). One-way ANOVA indicated that there was a significant effect of the number of repeats ($F_{4,30}$ = 6.4123, $P < 0.0007$). Post hoc analysis indicated that the level of luciferase activity for 11r was significantly lower than that for 6 ($P < 0.05$), 7 ($P < 0.01$), and 9r ($P < 0.05$; n = 7 in each group; Fig. 6g). In addition, two-way ANOVA indicated no significant interaction between the number of repeats with Hesr3 or the control vector ($F_{4,65}$ = 0.67, P = 0.62). The value of luciferase expression from the each CP-Luc/exon 15 construct (6, 7, 9, 10, and 11r) with empty vector compared in Figure 6b–g was measured from same samples as used in Figure 6a.

Localization of Hesr Family Members in Mouse Midbrain

We next analyzed the localization of Hesr1, -2, and -3 by immunoperoxidase staining. Hesr1-, Hesr2-, and Hesr3-ir cells were observed in both dopaminergic and nondopaminergic regions in the mouse midbrain (Fig. 7a). Immunoreactivity against Hesr1 and -2 was observed mainly in the nucleus, whereas Hesr3 was detected in the cytoplasm (Fig. 7b). However, in the nondopaminergic regions, immunoreactivity against Hesr1 and -2 was detected in the nucleus and cytoplasm (Fig. 7c). We also analyzed the localization of Hesr family members in the TH-ir cells using double-fluorescence immunostaining. Hesr1-, Hesr2-, and Hesr3-TH-ir cells were observed in both the SN and the VTA (Fig. 8).

DISCUSSION

Roles of the 3′-UTR Including VNTR Domain for *DAT* Expression

The relative luciferase activity of CP-Luc was significantly higher than that of CP-Luc/exon 15 (10r) in SH-SY5Y cells (Fig. 3). This suggests that the 3′-UTR plays an inhibitory role in *DAT1* expression. It is possible that endogenous factors affect *DAT1* expression via the 3′-UTR; in fact, it is predicted that more than one factor binds to this region (Michelhaugh et al., 2001). Thus, we investigated the HESR family as novel candidate regulatory factors modulating *DAT1* expression.

Effects of HESR Family on the *DAT* Core Promoter

Human HESR1 and -2 or mouse Hesr1, -2, and -3 significantly decreased the relative luciferase activity level of CP-Luc containing the *DAT1* core promoter, whereas human HESR3 increased CP-Luc activity (Fig. 4). These results were unexpected, insofar as HESR1 has been identified as a 3′-UTR-binding protein. This suggests that the HESR family generally down-regulates *DAT* expression through the core promoter region. In particular, HESR1 showed strong inhibitory effects in this region, with a 36% decrease in luciferase activity with human HESR1 expression and a 39% decrease with mouse Hesr1. In fact, the core promoter region has an E-box known to be bHLH-binding consensus sites. Moreover, it has been reported that mouse *Hesr2* does not contain an E- or N-box and is repressed by Hesr proteins (Nakagawa et al., 2000). Therefore, it is likely that HESR family members recognize a binding site different from that recognized by other bHLH family members. In addition, a functional single nucleotide polymorphism (SNP; −67 A/T) in the promoter was reported to be associated with personality traits, ADHD, and bipolar disorder (Greenwood and Kelsoe, 2003; Ohadi et al., 2006, 2007; Shibuya et al., 2009). This SNP may be a point of interaction with HESR family members.

Human HESR3 was the only HESR family member that significantly increased luciferase activity of CP-Luc containing the *DAT1* core promoter. We previously reported that HESR1 containing the Leu94Met SNP in the second helix of the bHLH domain lacked inhibitory activity (Fuke et al., 2005). It was also demonstrated that this SNP dramatically transforms HESR1 from an androgen receptor corepressor to an activator (Villaronga et al., 2010). HESR3 is the only HESR with a single-amino-acid substitution adjacent to the Leu in HESR1 and -2 located in the second helix of the bHLH domain (Fig. 2). Thus, the second helix in HESR family members may be critical in the modulation of gene expression.

Effects of HESR Family on the 3′-UTR of DAT

As shown in Figure 5, human and mouse HESR1 and -2 significantly inhibited the luciferase activity of CP-Luc/exon 15 (10r). Taken together with the results shown in Figure 4, this result indicates that HESR1 and

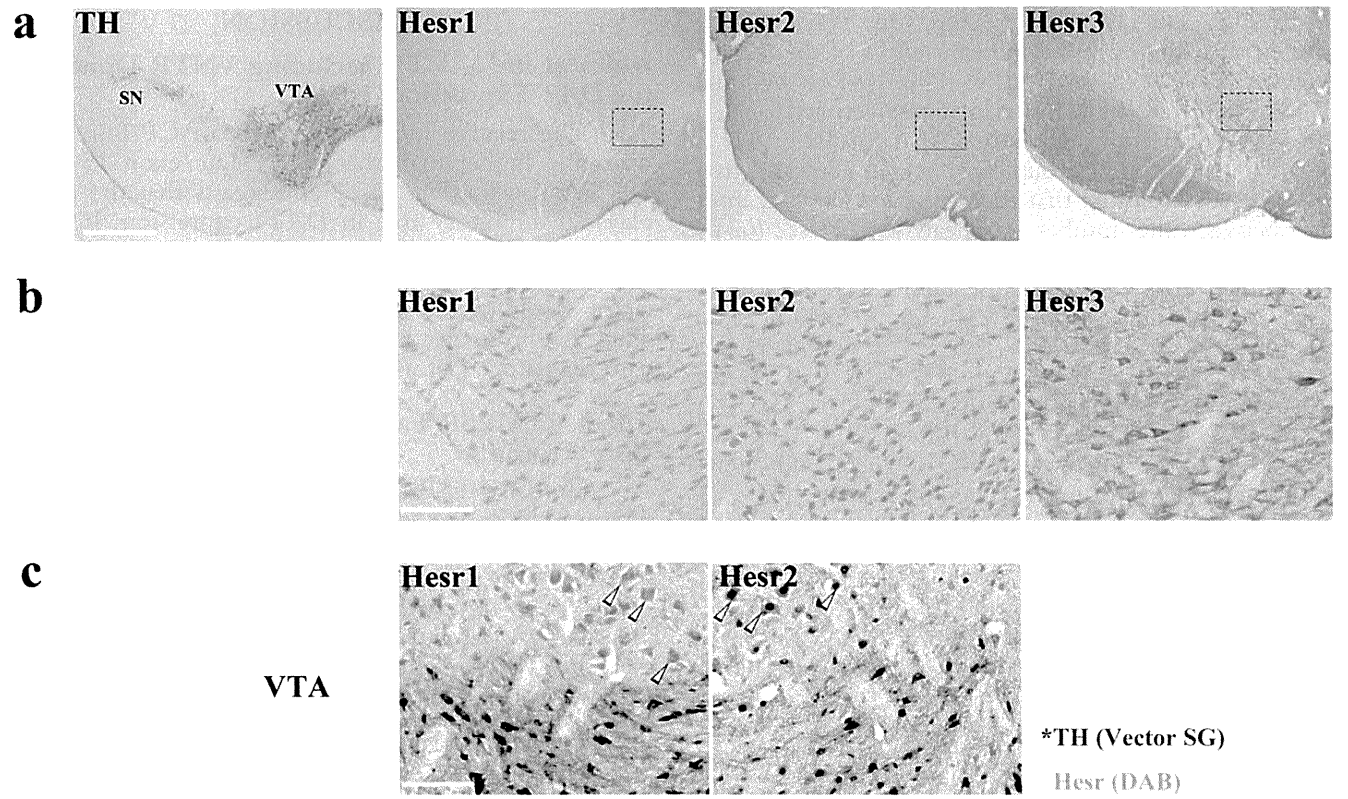

Fig. 7. Distribution of the Hesr family in mouse midbrain. Photomicrographs showing immunoperoxidase staining visualized by DAB (brown) or Vector SG (blue/gray). **a:** Localization of tyrosine hydroxylase (TH) or each Hesr family member in mouse midbrain, including the substantia nigra (SN) and ventral tegmental area (VTA). **b:** High-magnification images of the boxed areas in a. Hesr1 and -2 are localized primarily in the nucleus, whereas Hesr3 is located predominantly in the cytoplasm. **c:** Photomicrographs of the VTA and surrounding area depicting dual labeling for TH (Vector SG) and Hesr1 or 2 (DAB). Arrowheads indicate cells in which Hesr1 or -2 immunoreactivity was observed in both the nucleus and the cytoplasm. Scale bars = 500 μm in a; 100 μm in b,c.

-2 inhibit *DAT1* expression through both the core promoter and the 3′-UTR. HESR1 and -2 decreased the relative level of luciferase activity to less than 25% (HESR1) and 50% (HESR2). This degree of decrease is relatively high compared with that seen with the CP-Luc. Thus, HESR1 and -2 may have a stronger inhibitory effect on *DAT1* expression in the presence of the 3′-UTR.

We previously showed that HESR1 bound the 3′-UTR of *DAT1* directly by electromobility shift assays (Fuke et al., 2006). Because the bHLH domain is highly conserved (Steidl et al., 2000), we investigated the effect of other HESR family members to determine whether they affect gene expression by interacting with this same region. It has been proposed that more than one factor binds to this region and that the 3′-UTR, including the VNTR domain, modulates gene expression (Michelhaugh et al., 2001). Functional VNTR polymorphisms also exist in the serotonin transporter (*SERT*) gene located in intron 2, and two transcription factors, Y box-binding protein 1 (YB-1) and CCTC-binding factor (CTCF), were found to be responsible for the modulation of VNTR function (Klenova et al., 2004). This suggests that the VNTR domain functions as a modulator of gene expression (Nakamura et al., 1998) with other binding proteins.

Comparison of *DAT* Expression With the VNTR: Differential Effects of HESR Family on Each VNTR Allele

The number of repeats in the VNTR domain significantly affected the level of luciferase activity of CP-Luc/exon 15 in SH-SY5Y cells (Fig. 6a). This suggests that the VNTR domain in the *DAT* 3′-UTR is the functional sequence for *DAT* expression and is supported by in vivo neuroimaging involving SPECT (Heinz et al., 2000; Jacobsen et al., 2000; Martinez et al., 2001) and ex vivo RT-PCR analysis (Mill et al., 2002; Brookes et al., 2007). When the HESR family was transiently transfected, the number of repeats in the VNTR domain significantly affected the luciferase activity of CP-Luc/exon 15 (Fig. 6b–g). In addition, interactive effects between the number of repeats and the HESR or control vector were detected for all groups except mouse Hesr3. This suggests that the HESR

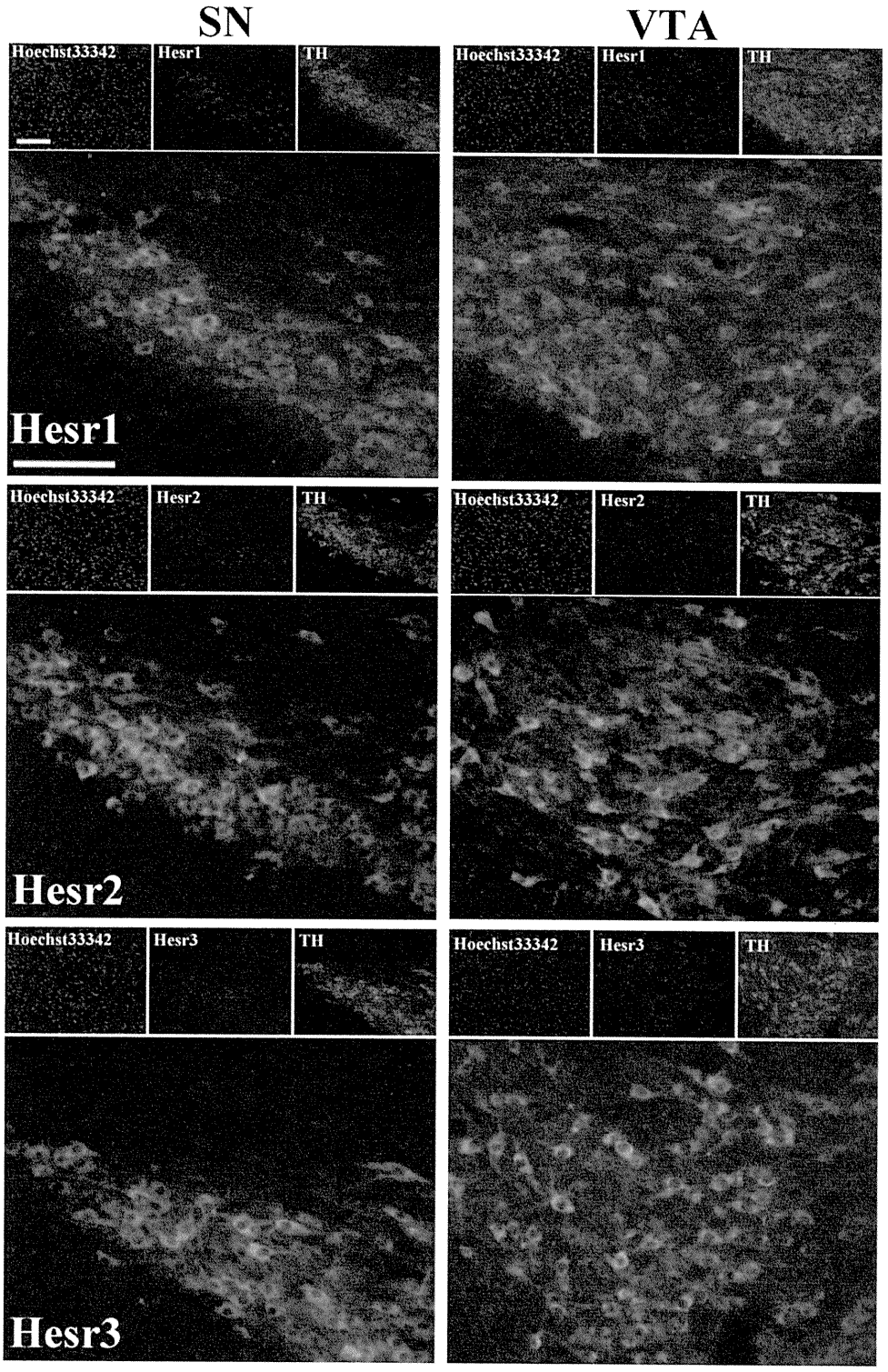

Fig. 8. Colocalization of Hesr family proteins with dopaminergic neurons. Fluorescence immunohistochemical analysis of the Hesr family protein and tyrosine hydroxylase (TH) distribution in the substantia nigra (SN) and ventral tegmental area (VTA). Hesr, magenta (Cy3); TH, green (Cy2); Hoechst 33342, blue. Scale bars = 100 μm.

family, or at least HESR1 and -2, differentially alter *DAT1* expression depending on the VNTR allele. This supports our idea that cell-specific factors regulate *DAT1* expression in a VNTR allele-specific manner and may explain the discrepancies among previous studies (D'souza and Craig, 2008).

Functional Considerations

We first reported the functional significance of the *DAT* VNTR sequence at the molecular level using luciferase reporter assays (Fuke et al., 2001). After our report, other groups reported interesting but conflicting in vitro results (Fuke et al., 2001, 2005; Inoue-Murayama et al., 2002; Miller and Madras, 2002; Greenwood and Kelsoe, 2003; VanNess et al., 2005; Mill et al., 2005; D'souza and Craig, 2008). One explanation for this is that different promoters and cell lines were used in each study. In fact, our previous study (Fuke et al., 2005) revealed that the inhibitory effect of the *DAT* 3′-UTR in CP-Luc/exon15 was not detected in HEK293 cells, but we could detected it in SH-SY5Y, Neuro2A, and COS-7 cell lines. Every cell line might not express all the transcription factors necessary for regulation of the *DAT1* gene, as D'souza and Craig (2008) speculated. Thus, the identification of the regulating factor for *DAT1* was necessary. We previously identified HESR1 as a 3′-UTR-binding protein using a yeast one-hybrid system (Fuke et al., 2005) and showed that HESR1 inhibited the luciferase activity of CP-Luc/exon 15 in SY-SY5Y, Neuro2A, COS-7, and also HEK293 cells. This indicates that HESR1 may regulate *DAT1* expression.

We also reported the increased expression of *DAT* in the brains of *Hesr1* KO mice. These mice also showed a decrease in spontaneous locomotor activity and a reduction in exploration of novelty (Fuke et al., 2006). This is consistent with our previous and present results, insofar as HESR1 is thought to be a *DAT*-inhibitory factor. In addition, the expression of several dopamine receptor genes (*DRD1*, *DRD2*, *DRD4*, and *DRD5*), the main targets of synaptic dopamine responsiveness, were enhanced in *Hesr1* KO mice. These phenomena are in contrast to what is seen in *DAT* KO mice. Mice lacking *DAT* show decreased intraneural dopamine storage and spontaneous hyperlocomotion following the down-regulation of several dopamine-related genes, including those encoding dopamine receptors D1 and D2 (Giros et al., 1996; Caine, 1998; Jaber et al., 1999; Fauchey et al., 2000; Gainetdinov et al., 2002). This result highlights the importance of Hesr1 in the dopaminergic system in vivo and suggests that further investigation of the in vivo functions of Hesr2 and -3 is needed.

The *Hesr1/2* double mutation is known to be embryonic lethal as a result of cardiac and vascular dysplasia, and both genes have been shown to be involved in neural development (Sakamoto et al., 2003; Fischer et al., 2004; Kokubo et al., 2005). However, whereas *Hesr2* KO mice exhibited heart dysfunction (Kokubo et al., 2004), *Hesr1* KO mice exhibited no obvious morphological or anatomical phenotype (Fischer et al., 2004; Kokubo et al., 2005). On the other hand, interactions between *Hesr1* and transforming growth factor-β (TGF-β) or bone morphogenetic protein (BMP) signaling (Dahlqvist et al., 2003; Takizawa et al., 2003; Zavadil et al., 2004), which functions in the differentiation and maintenance of the dopaminergic nervous system, have been reported (Stull et al., 2001; Farkas et al., 2003; Sanchez-Capelo et al., 2003). *HESR1* may play important roles in the dopaminergic nervous system and the regulation of *DAT*. *HESR* family genes encode a bHLH domain that is essential for DNA binding, an Orange domain and YRPW motif. HESR proteins dimerize with other bHLH proteins via the bHLH domain and bind to corepressors via the YRPW motif (Fischer and Gessler, 2007). Additional investigations are needed to characterize these interacting proteins. In the present study, the results obtained for HESR3 sometimes differed from those obtained for HESR1 and -2. One possible reason for this is the lack of a YRPW motif in HESR3 (Fig. 2).

Our findings may lead to novel therapies for DAT-related disorders. In the case of SERT, YB-1 and CTCF act as regulators of SERT (Klenova et al., 2004) and are targeted by lithium chloride, a mood stabilizer that modifies CTCF and YB-1 expression (Roberts et al., 2007).

DAT gene is expressed exclusively in the dopaminergic neurons (Uhl, 2003). If Hesr family genes are not expressed in the dopaminergic neurons, Hesrs cannot inhibit *DAT* expression via 3′-UTR of DAT. However, as shown in Figures 7 and 8, each Hesr was expressed in dopaminergic neurons throughout the SN and VTA. This suggests that the HESR family influences *DAT* expression in vivo, as observed in our present culture studies. At the same time, these data suggest that HESR family members are involved in mesostriatal and mesocorticolimbic dopamine systems underlying motor control, emotion, and cognition (Bjorklund and Dunnett, 2007).

In a study of prostate cancer, HESR1 was reported to be an androgen receptor-interacting factor (Belandia et al., 2005). It has also been shown that HESR1 is excluded from the nucleus in most human prostate cancers, raising the possibility that abnormal HESR1 subcellular distribution plays a role in the aberrant hormonal responses observed in prostate cancer. In the present study, as shown in Figure 7c, Hesr1 and -2 were localized not only to the nucleus but also to the cytoplasm of nondopaminergic cells in the brain. Thus, the cellular localization of HESR family members may be important for some physiological functions or pathological conditions and warrants further study.

Although it seems clear that the VNTR domain plays a role in regulating *DAT* expression in vitro, there are discrepancies in the proposed differential effects of the various alleles. In vivo studies using transgenic mice with *DAT-9r* or *10r* knock-ins may facilitate the characterization of the mechanisms underlying *DAT* transcriptional regulation. The mouse Hesr data presented here will serve as a molecular basis for generating these animals.

In conclusion, we have demonstrated the differential expression of a luciferase reporter vector containing the *DAT1* 3′-UTR and VNTR domain as well as the differential inhibitory effects of HESR family members on *DAT1* expression via the VNTR domain. Given these findings, additional behavioral and psychiatric studies of personality should be conducted.

ACKNOWLEDGMENTS

We thank Dr. H. Kokubo (National Institute of Genetics) for kindly providing the mouse Hesr constructs and Dr. M.J. Bannon (Wayne State University) for kindly providing us with the DAT1-8317 plasmid. We also thank our former colleagues S. Fuke (RIKEN BSI), O.-A. Asami (University of California, Los Angeles), and K. Toriumi (Meijo University) for technical advice and encouragement. We thank Dr. S. Tsukahara (Saitama University), A. Ito (University of Tokyo), S. Yamada (Kyoto Prefectural University of Medicine), and H. Ito (Weseda University) for technical advice regarding immunohistochemistry. The authors declare no conflict of interest.

REFERENCES

Bannon MJ, Michelhaugh SK, Wang J, Sacchetti P. 2001. The human dopamine transporter gene: gene organization, transcriptional regulation, and potential involvement in neuropsychiatric disorders. Eur Neuropsychopharmacol 11:449–455.

Belandia B, Powell SM, Garcia-Pedrero JM, Walker MM, Bevan CL, Parker MG. 2005. Hey1, a mediator of notch signaling, is an androgen receptor corepressor. Mol Cell Biol 25:1425–1436.

Bjorklund A, Dunnett SB. 2007. Dopamine neuron systems in the brain: an update. Trends Neurosci 30:194–202.

Brookes KJ, Neale BM, Sugden K, Khan N, Asherson P, D'souza UM. 2007. Relationship between VNTR Polymorphisms of the human dopamine transporter gene and expression in post-mortem midbrain tissue. Am J Med Genet B Neuropsychiatr Genet 144B:1070–1078.

Brunswick DJ, Amsterdam JD, Mozley PD, Newberg A. 2003. Greater availability of brain dopamine transporters in major depression shown by Tc-^{99}m TRODAT-1 SPECT imaging. Am J Psychiatry 160:1836–1841.

Caine SB. 1998. Cocaine abuse: hard knocks for the dopamine hypothesis? Nat Neurosci 1:90–92.

Cook EH, Stein MA, Krasowski MD, Cox NJ, Olkon DM, Kieffer JE, Leventhal BL. 1995. Association of attention-deficit disorder and dopamine transporter gene. Am J Hum Genet 56:993–998.

D'souza UM, Craig IW. 2008. Functional genetic polymorphisms in serotonin and dopamine gene systems and their significance in behavioural disorders. Prog Brain Res 172:73–98.

Dahlqvist C, Blokzijl A, Chapman G, Falk A, Dannaeus K, Ibanez CF, Lendahl U. 2003. Functional notch signaling is required for BMP4-induced inhibition of myogenic differentiation. Development 130:6089–6099.

Farkas LM, Dunker N, Roussa E, Unsicker K, Krieglstein K. 2003. Transforming growth factor-beta s are essential for the development of midbrain dopaminergic neurons in vitro and in vivo. J Neurosci 23:5178–5186.

Fauchey V, Jaber M, Caron MG, Bloch B, Le Moine C. 2000. Differential regulation of the dopamine D1, D2 and D3 receptor gene expression and changes in the phenotype of the striatal neurons in mice lacking the dopamine transporter. Eur J Neurosci 12:19–26.

Fischer A, Gessler M. 2007. Delta-Notch-and then? Protein interactions and proposed modes of repression by Hes and Hey bHLH factors. Nucleic Acids Res 35:4583–4596.

Fischer A, Schumacher N, Maier M, Sendtner M, Gessler M. 2004. The Notch target genes Hey1 and Hey2 are required for embryonic vascular development. Gene Dev 18:901–911.

Franklin KBJ, Paxinos G. 2008. The mouse brain in stereotaxic coordinates. Amsterdam: Elsevier/Academic Press.

Fuke S, Suo S, Takahashi N, Koike H, Sasagawa N, Ishiura S. 2001. The VNTR polymorphism of the human dopamine transporter (*DAT1*) gene affects gene expression. Pharmacogenomics J 1:152–156.

Fuke S, Sasagawa N, Ishiura S. 2005. Identification and characterization of the Hesr1/Hey1 as a candidate trans-acting factor on gene expression through the 3′ non-coding polymorphic region of the human dopamine transporter (*DAT1*) gene. J Biochem 137:205–216.

Fuke S, Minami N, Kokubo H, Yoshikawa A, Yasumatsu H, Sasagawa N, Saga Y, Tsukahara T, Ishiura S. 2006. Hesr1 knockout mice exhibit behavioral alterations through the dopaminergic nervous system. J Neurosci Res 84:1555–1563.

Gainetdinov RR, Sotnikova TD, Caron MG. 2002. Monoamine transporter pharmacology and mutant mice. Trends Pharmacol Sci 23:367–373.

Giros B, Caron MG. 1993. Molecular characterization of the dopamine transporter. Trends Pharmacol Sci 14:43–49.

Giros B, Elmestikawy S, Bertrand L, Caron MG. 1991. Cloning and functional characterization of a cocaine-sensitive dopamine transporter. FEBS Lett 295:149–154.

Giros B, Elmestikawy S, Godinot N, Zheng KQ, Han H, Yangfeng T, Caron MG. 1992. Cloning, pharmacological characterization, and chromosome assignment of the human dopamine transporter. Mol Pharmacol 42:383–390.

Giros B, Jaber M, Jones SR, Wightman RM, Caron MG. 1996. Hyperlocomotion and indifference to cocaine and amphetamine in mice lacking the dopamine transporter. Nature 379:606–612.

Greenwood TA, Kelsoe JR. 2003. Promoter and intronic variants affect the transcriptional regulation of the human dopamine transporter gene. Genomics 82:511–520.

Heinz A, Goldman D, Jones DW, Palmour R, Hommer D, Gorey JG, Lee KS, Linnoila M, Winberger DR. 2000. Genotype influences in vivo dopamine transporter availability in human striatum. Neuropsychopharmacology 22:133–139.

Henderson AM, Wang SJ, Taylor AC, Aitkenhead M, Hughes CCW. 2001. The basic helix-loop-helix transcription factor HESR1 regulates endothelial cell tube formation. J Biol Chem 276:6169–6176.

Inoue-Murayama M, Adachi S, Mishima N, Mitani H, Takenaka O, Terao K, Hayasaka I, Ito S, Murayama Y. 2002. Variation of variable number of tandem repeat sequences in the 3′-untransiated region of primate dopamine transporter genes that affects reporter gene expression. Neurosci Lett 334:206–210.

Iso T, Sartorelli V, Poizat C, Iezzi S, Wu HY, Chung G, Kedes L, Hamamori Y. 2001. HERP, a novel heterodimer partner of HES/E(spl) in notch signaling. Mol Cell Biol 21:6080–6089.

Iso T, Kedes L, Hamamori Y. 2003. HES and HERP families: Multiple effectors of the Notch signaling pathway. J Cell Physiol 194:237–255.

Jaber M, Dumartin B, Sagne C, Haycock JW, Roubert C, Giros B, Bloch B, Caron MG. 1999. Differential regulation of tyrosine hydroxylase in the basal ganglia of mice lacking the dopamine transporter. Eur J Neurosci 11:3499–3511.

Jackson DM, Westlinddanielsson A. 1994. Dopamine receptors: molecular biology, biochemistory and behavioral aspects. Pharmacol Ther 64:291–370.

Jacobsen LK, Staley JK, Zoghbi S, Seibyl JP, Kosten TR, Innis RB, Gelernter J. 2000. Prediction of dopamine transporter binding availability by genotype: a preliminary report. Am J Psychiatry 157:1700–1703.

Kilty JE, Lorang D, Amara SG. 1991. Cloning and expression of a cocaine-sensitive rat dopamine transporter. Science 254:578–579.

Klenova E, Scott AC, Roberts J, Shamsuddin S, Lovejoy EA, Bergmann S, Bubb VJ, Royer HD, Quinn JP. 2004. YB-1 and CTCF differentially regulate the 5-HTT polymorphic intron 2 enhancer which predisposes to a variety of neurological disorders. J Neurosci 24:5966–5973.

Kokubo H, Lun Y, Johnson RL. 1999. Identification and expression of a novel family of bHLH cDNAs related to *Drosophila* hairy and enhancer of split. Biochem Biophys Res Commun 260:459–465.

Kokubo H, Miyagawa-Tomita S, Tomimatsu H, Nakashima Y, Nakazawa M, Saga Y, Johnson RL. 2004. Targeted disruption of hesr2 results in atrioventricular valve anomalies that lead to heart dysfunction. Circ Res 95:540–547.

Kokubo H, Miyagawa-Tomita S, Nakazawa M, Saga Y, Johnson RL. 2005. Mouse hesr1 and hesr2 genes are redundantly required to mediate Notch signaling in the developing cardiovascular system. Dev Biol 278:301–309.

Kokubo H, Tomita-Miyagawa S, Hamada Y, Saga Y. 2007. Hesr1 and Hesr2 regulate atrioventricular boundary formation in the developing heart through the repression of Tbx2. Development 134:747–755.

Kouzmenko AP, Pereira AM, Singh BS. 1997. Intronic sequences are involved in neural targeting of human dopamine transporter gene expression. Biochem Biophys Res Commun 240:807–811.

Krause KH, Dresel SH, Krause J, la Fougere C, Ackenheil M. 2003. The dopamine transporter and neuroimaging in attention deficit hyperactivity disorder. Neurosci Biobehav Rev 27:605–613.

Leimeister C, Externbrink A, Klamt B, Gessler M. 1999. Hey genes: a novel subfamily of hairy- and Enhancer of split related genes specifically expressed during mouse embryogenesis. Mech Dev 85:173–177.

Madras BK, Gracz LM, Fahey MA, Elmaleh D, Meltzer PC, Liang AY, Stopa EG, Babich J, Fischman AJ. 1998. Altropane, a SPECT or PET imaging probe for dopamine neurons: III. Human dopamine transporter in postmortem normal and Parkinson's diseased brain. Synapse 29:116–127.

Martinez D, Gelernter J, Abi-Dargham A, van Dyck CH, Kegeles L, Innis RB, Laruelle M. 2001. The variable number of tandem repeats polymorphism of the dopamine transporter gene is not associated with significant change in dopamine transporter phenotype in humans. Neuropsychopharmacology 24:553–560.

Michelhaugh SK, Fiskerstrand C, Lovejoy E, Bannon MJ, Quinn JP. 2001. The dopamine transporter gene (SLC6A3) variable number of tandem repeats domain enhances transcription in dopamine neurons. J Neurochem 79:1033–1038.

Mill J, Asherson P, Browes C, D'souza U, Craig I. 2002. Expression of the dopamine transporter gene is regulated by the 3′ UTR VNTR: evidence from brain and lymphocytes using quantitative RT-PCR. Am J Med Genet B Neuropsychiatr Genet 114B:975–979.

Mill J, Asherson P, Craig I, D'souza UM. 2005. Transient expression analysis of allelic variants of a VNTR in the dopamine transporter gene (*DAT1*). BMC Genet 6.

Miller GM, Madras BK. 2002. Polymorphisms in the 3′-untranslated region of human and monkey dopamine transporter genes affect reporter gene expression. Mol Psychiatry 7:44–55.

Missale C, Nash SR, Robinson SW, Jaber M, Caron MG. 1998. Dopamine receptors: From structure to function. Physiol Rev 78:189–225.

Muller-Vahl KR, Berding G, Brucke T, Kolbe H, Meyer GJ, Hundeshagen H, Dengler R, Knapp WH, Emrich HM. 2000. Dopamine transporter binding in Gilles de la Tourette syndrome. J Neurol 247:514–520.

Nakagawa O, Nakagawa M, Richardson JA, Olson EN, Srivastava D. 1999. HRT1, HRT2, and HRT3: a new subclass of bHLH transcription factors marking specific cardiac, somitic, and pharyngeal arch segments. Dev Biol 216:72–84.

Nakagawa O, McFadden DG, Nakagawa M, Yanagisawa H, Hu TH, Srivastava D, Olson EN. 2000. Members of the HRT family of basic helix-loop-helix proteins act as transcriptional repressors downstream of Notch signaling. Proc Natl Acad Sci U S A 97:13655–13660.

Nakamura Y, Koyama K, Matsushima M. 1998. VNTR (variable number of tandem repeat) sequences as transcriptional, translational, or functional regulators. J Hum Genet 43:149–152.

Ohadi M, Shirazi E, Tehranidoosti M, Moghimi N, Keikhaee MR, Ehssani S, Aghajani A, Najrnabadi H. 2006. Attention-deficit/hyperactivity disorder (ADHD) association with the *DAT1* core promoter-67 T allele. Brain Res 1101:1–4.

Ohadi M, Keikhaee MR, Javanbakht A, Sargolzaee MR, Robabeh M, Najmabadi H. 2007. Gender dimorphism in the DAT1–67 T-allele homozygosity and predisposition to bipolar disorder. Brain Res 1144:142–145.

Roberts J, Scott AC, Howard MR, Breen G, Bubb VJ, Klenova E, Quinn JP. 2007. Differential regulation of the serotonin transporter gene by lithium is mediated by transcription factors, CCCTC binding protein and Y-box binding protein 1, through the polymorphic intron 2 variable number tandem repeat. J Neurosci 27:2793–2801.

Sacchetti P, Brownschidle LA, Granneman GJ, Bannon MJ. 1999. Characterization of the 5′-flanking region of the human dopamine transporter gene. Brain Res Mol Brain Res 74:167–174.

Sakamoto M, Hirata H, Ohtsuka T, Bessho Y, Kageyama R. 2003. The basic helix-loop-helix genes Hesr1/Hey1 and Hesr2/Hey2 regulate maintenance of neural precursor cells in the brain. J Biol Chem 278:44808–44815.

Sanchez-Capelo A, Colin P, Guibert B, Biguet NF, Mallet J. 2003. Transforming growth factor beta 1 overexpression in the nigrostriatal system increases the dopaminergic deficit of MPTP mice. Mol Cell Neurosci 23:614–625.

Shibuya N, Kamata M, Suzuki A, Matsumoto Y, Goto K, Otani K. 2009. The-67 A/T promoter polymorphism in the dopamine transporter gene affects personality traits of Japanese healthy females. Behav Brain Res 203:23–26.

Shimada S, Kitayama S, Lin CL, Patel A, Nanthakumar E, Gregor P, Kuhar M, Uhl G. 1991. Cloning and expression of a cocaine-sensitive dopamine transporter complementary DNA. Science 254:576–578.

Steidl C, Leimeister C, Klamt B, Maier M, Nanda I, Dixon M, Clarke R, Schmid M, Gessler M. 2000. Characterization of the human and mouse HEY1, HEY2, and HEYL genes: Cloning, mapping, and mutation screening of a new bHLH gene family. Genomics 66:195–203.

Stull ND, Jung JW, Iacovitti L. 2001. Induction of a dopaminergic phenotype in cultured striatal neurons by bone morphogenetic proteins. Brain Res Dev Brain Res 130:91–98.

Takizawa T, Ochiai W, Nakashima K, Taga T. 2003. Enhanced gene activation by Notch and BMP signaling cross-talk. Nucleic Acids Res 31:5723–5731.

Ueno S. 2003. Genetic polymorphisms of serotonin and dopamine transporters in mental disorders. J Med Invest 50:25–31.

Ueno S, Nakamura M, Mikami M, Kondoh K, Ishiguro H, Arinami T, Komiyama T, Mitsushio H, Sano A, Tanabe H. 1999. Identification of a novel polymorphism of the human dopamine transporter (*DAT1*) gene and the significant association with alcoholism. Mol Psychiatry 4:552–557.

Uhl GR. 2003. Dopamine transporter: Basic science and human variation of a key molecule for dopaminergic function, locomotion, and parkinsonism. Mov Disord 18:S71–S80.

Vandenbergh DJ, Persico AM, Hawkins AL, Griffin CA, Li X, Jabs EW, Uhl GR. 1992. Human dopamine transporter gene (*DAT1*) maps to chromosome 5p15.3 and displays a VNTR. Genomics 14:1104–1106.

Vandenbergh DJ, Thompson MD, Cook EH, Bendahhou E, Nguyen T, Krasowski MD, Zarrabian D, Comings D, Sellers EM, Tyndale RF, George SR, O'Dowd BF, Uhl GR. 2000. Human dopamine transporter gene: coding region conservation among normal, Tourette's disorder, alcohol dependence and

attention-deficit hyperactivity disorder populations. Mol Psychiatry 5:283–292.

VanNess SH, Owens MJ, Kilts CD. 2005. The variable number of tandem repeats element in DATI regulates in vitro dopamine transporter density. BMC Genet 6.

Villaronga MA, Lavery DN, Bevan CL, Llanos S, Belandia B. 2010. HEY1 Leu94Met gene polymorphism dramatically modifies its biological functions. Oncogene 29:411–420.

Wang WL, Campos AH, Prince CZ, Mou YS, Pollman MJ. 2002. Coordinate Notch3-hairy-related transcription factor pathway regulation in response to arterial injury—mediator role of platelet-derived growth factor and ERK. J Biol Chem 277:23165–23171.

Zavadil J, Cermak L, Soto-Nieves N, Bottinger EP. 2004. Integration of TGF-beta/Smad and Jagged1/Notch signalling in epithelial-to-mesenchymal transition. EMBO J 23:1155–1165.

The FASEB Journal • Research Communication

An alternative metabolic pathway of amyloid precursor protein C-terminal fragments *via* cathepsin B in a human neuroglioma model

Masashi Asai,*[,†,1,2] Sosuke Yagishita,[‡,2,3] Nobuhisa Iwata,[†,§] Takaomi C. Saido,[†] Shoichi Ishiura,[‡] and Kei Maruyama*

*Department of Pharmacology, Faculty of Medicine, Saitama Medical University, Saitama, Japan; [†]Laboratory for Proteolytic Neuroscience, RIKEN Brain Science Institute, Saitama, Japan; [‡]Department of Life Sciences, Graduate School of Arts and Sciences, The University of Tokyo, Tokyo, Japan; and [§]Graduate School of Biomedical Sciences, Nagasaki University, Nagasaki, Japan

ABSTRACT **γ-Secretase catalyzes the cleavage of the intramembrane region of the Alzheimer amyloid precursor protein (APP), generating p3, amyloid-β peptide (Aβ), and the APP intracellular domain (AICD). Although a γ-secretase inhibitor has been shown to cause an accumulation of the APP C-terminal fragments (CTFs) α and β and to decrease levels of p3 or Aβ and AICD, we found that treatment with a lysosomotropic weak base, such as chloroquine or ammonium chloride, caused simultaneous accumulation of both CTFs and AICD, suggesting that lysosomal proteases are also involved in processing of APP. This observation was reinforced by the results that cysteine protease inhibitor E-64d and cathepsin B specific inhibitor CA-074Me caused the accumulation of both CTFs and AICD with no change in known secretase activities. γ-Secretase preferentially cleaved phosphorylated CTFs to produce Aβ, but cathepsin B degraded CTFs regardless of phosphorylation. Our results suggest that cathepsin B plays novel roles in the metabolism of APP and that an inhibition of APP phosphorylation is an attractive therapeutic target for Alzheimer's disease.—Asai, M., Yagishita, S., Iwata, N., Saido, T. C., Ishiura, S., Maruyama, K. An alternative metabolic pathway of amyloid precursor protein C-terminal fragments *via* cathepsin B in a human neuroglioma model. *FASEB J.* 25, 3720–3730 (2011). www.fasebj.org**

Key Words: Alzheimer's disease · CA-074Me · γ-secretase · phosphorylation

AMYLOID PRECURSOR PROTEIN (APP) is a type I integral membrane glycoprotein with a single membrane-spanning domain, a large ectoplasmic N-terminal region, and a shorter cytoplasmic C-terminal region (1–3). An understanding of APP metabolism is physiologically and clinically important because APP is a stepwise substrate for β- and γ-secretases in the production of the neurotoxic amyloid-β peptide (Aβ; Aβ40 or Aβ42; refs. 1–4). Thus, β- and γ-secretase inhibitors are pharmacological targets for the treatment or prevention of Alzheimer's disease (AD; refs. 4, 5).

Proteolytic processing of APP has been extensively studied, and two major processing pathways have been described. Initially, α- or β-secretase cleaves APP to produce a secreted N-terminal soluble extracellular fragment of APP (sAPPα or sAPPβ) and membrane-bound C-terminal fragments of APP (CTFα or CTFβ). Sequentially, γ-secretase catalyzes the intramembrane proteolysis of CTFs to produce p3, Aβ, and APP intracellular domain (AICD; refs. 1–4).

Numerous γ-secretase inhibitors have been developed (2, 4, 5), and treatment with a γ-secretase inhibitor causes accumulation of substrates, such as CTFs, and suppression of the production of Aβ and AICD *in vivo* or *in vitro* (6–9). This quantitative balance of CTFs, Aβ, and AICD seems to be dependent on γ-secretase, which is an enzymatic multiprotein complex containing presenilin (PS; either PS1 or PS2) as the active core. However, it has been reported that both CTFs and AICD simultaneously accumulated under treatment with lysosomotropic weak bases, such as chloroquine or ammonium chloride (NH_4Cl; refs. 10, 11). It is highly unlikely that alkalization of the endosome-lysosome system causes γ-secretase dysfunction because γ-secretase can cleave other substrates, such as Notch, and can produce intracellular fragments in the presence of these lysosomal inhibitors. In other words, the accumulation of both products and substrates of γ-secretase is indicative of the presence of proteases other than γ-secretase for the processing of CTFs and AICD.

To identify CTF- and AICD-processing enzymes, we analyzed APP metabolism using a pharmacological

[1] Correspondence: Department of Pharmacology, Faculty of Medicine, Saitama Medical University, 38 Moro-hongo, Moroyama-machi, Iruma-gun, Saitama 350-0495, Japan. E-mail: asai@saitama-med.ac.jp

[2] These authors contributed equally to this work.

[3] Current address: Laboratory for Alzheimer's Disease, RIKEN Brain Science Institute, Saitama, Japan.

doi: 10.1096/fj.11-182154

This article includes supplemental data. Please visit *http://www.fasebj.org* to obtain this information.

0892-6638/11/0025-3720 © FASEB